Membrane properties of sodium 2- and 6-(poly)prenyl-substituted polyprenyl phosphates

Saho Takajo,[a] Hajime Nagano,*[a] Olivier Dannenmuller,[b] Sangita Ghosh,[b] Anne Marie Albrecht,[c] Yoichi Nakatani*[b] and Guy Ourisson[b]

[a] *Department of Chemistry, Faculty of Science, Ochanomizu University, Otsuka, Bunkyo-ku, Tokyo 112-8610, Japan. E-mail: nagano@cc.ocha.ac.jp; Fax: +81-3-5978-5715*

[b] *Laboratoire de Chimie Organique des Substances Naturelles associé au CNRS, Centre de Neurochimie, Université Louis Pasteur, 5 rue Blaise Pascal, F-67084 Strasbourg, France. E-mail: nakatani@chimie.u-strasbg.fr; Fax: +33 3 88 60 76 20*

[c] *Ecole Européenne de Chimie, Polymères et Matériaux, Laboratoire de Physico-Chimie Bio-inorganique associé au CNRS, Institut de Chimie, 1 rue Blaise Pascal, F-67070 Strasbourg, France*

Received (in Montpellier, France) 26th February 2001, Accepted 11th April 2001
First published as an Advance Article on the web 19th June 2001

The amphiphilic 2- and 6-(poly)prenyl-substituted polyprenyl phosphates and their isomers, spontaneously form vesicles. Vesicle formation depends on the pH of the buffer and the structural features of the hydrophobic chains such as their lengths and the double bond positions. The compactness of the vesicles was estimated by measuring their water permeability, evaluating the intramolecular attractive van der Waals forces between the highly branched chains and measuring the spin–lattice relaxation times in ^{13}C NMR spectra.

1 Introduction

All known living organisms are cellular and the inside of each cell is separated from the outside by a thin water-insoluble membrane formed by the self-assembly of amphiphilic molecules. Except for Archaea, cell membranes of extant organisms are built of ester phospholipids with *n*-acyl chains (C_{14}–C_{18}), or often, in bacteria, with branched chains. However, polyprenyl phosphates could have been involved in the prebiotic formation of the most primitive membranes.[1,2] Terpenoids are ubiquitous and very varied in biological membranes of all the living organisms, either as structural constituents (polyprenyl phospholipid ethers in Archaea) or as mechanical reinforcers (hopanoids and carotenoids in Procarya; sterols in bacteria).[3] Furthermore, in contrast to *n*-acyl chains, terpenoids, normally biosynthesized by a series of enzymatic reactions, can be obtained under extremely simple conditions such as acid-catalyzed reactions, from simple molecules.[1,4]

We have shown that monopolyprenyl and dipolyprenyl phosphates (**1** and **2**) indeed form vesicles, provided the polyprenyl chains contain at least three prenyl units, as in **1** ($n = 1$ or 2) and **2** ($m + n \geqslant 1$).[2] Furthermore, we have postulated that the highly branched isoprenoid alkanes and alkenes **3** (C_{20}, C_{25}, C_{30} and C_{35}), which are distributed widely and abundantly in many sediments,[5] may have been derived from the corresponding polyprenylated polyprenyl amphiphiles **5** present in biomembranes in primitive organisms. The recent isolation of the branched isoprenoid hydrocarbons **3** and of their isomers **4** from diatomaceous algae[6] also suggests that the corresponding alcohols must still exist on Earth[7,8] at least as biosynthetic intermediates (Fig. 1).

We have recently synthesized a series of 2- and 6-(poly) prenyl-substituted polyprenyl phosphates and their isomers as their sodium salts **6**–**22**, possessing a hydrophobic portion of about 20 Å in length, one half of the thickness of all known biomembranes or shorter[9] (Fig. 2). We now report the pH dependence of the spontaneous formation of vesicles from these amphiphilic molecules (observed by optical microscopy) and their water permeability as an index of the compactness of their membranes. We also estimated the intramolecular attractive van der Waals forces between the hydrophobic chains of the alcohols corresponding to these phosphates and their mobility on the basis of ^{13}C spin lattice relaxation time measurements.

2 Materials and methods

2.1 Differential interference contrast microscopy, phase contrast microscopy and image analysis

Inverted optical microscope (Axiovert 135, 63 × /1.40 Plan Achromat Oil DIC objective, × 2.5 insertion lens, Carl Zeiss), light sources: Hg (HBO 100, bandpass 450–490 blue filter, bandpass 546–558 green filter, Carl Zeiss) and halogen lamp (12 V, 100 W, Carl Zeiss), charge-coupled device (CCD) camera (C 2400-75 H, Hamamatsu Photonics), image processor (Argus 20, Hamamatsu Photonics), S-VHS video recorder (SVO-9500 MDP, Sony), Trinitron color video monitor (PVM-1443 MD, Sony), microcomputer (Power MacIntosh 7500/100, Apple), video printer (VP-1800 EPM, Sony) and digital image recorder (Focus). Improvement of the optical microscopy image quality is achieved by increasing the ratio optical signal : background noise, by use of appropriate softwares (M.I.H. Image 1.55 and Photoshop 4.0).

Preparation and observation of vesicles. A typical procedure was as follows. A phosphate (3 mg) was dissolved in 300 μl of 2 : 1 (v/v) chloroform–methanol. An aliquot (15 μl) of the solution was dropped on a coverglass (0.17 mm thick). After 10 min of drying at room temperature, the lamellar solid remaining on the slide was brought into focus and 500 μl of a buffer at 25 °C were added (pH 3.1, 4.0 and 4.5: sodium acetate–

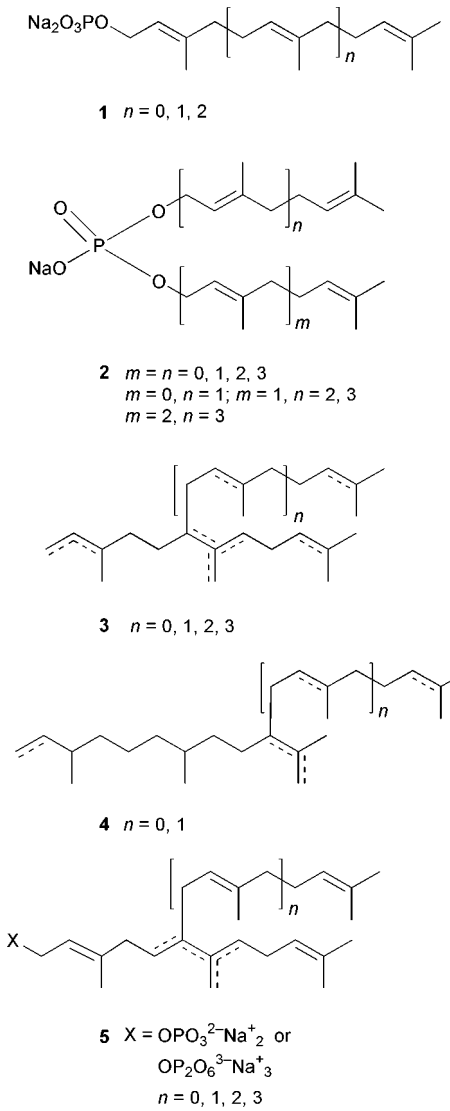

Fig. 1 Structures of **1**–**5**.

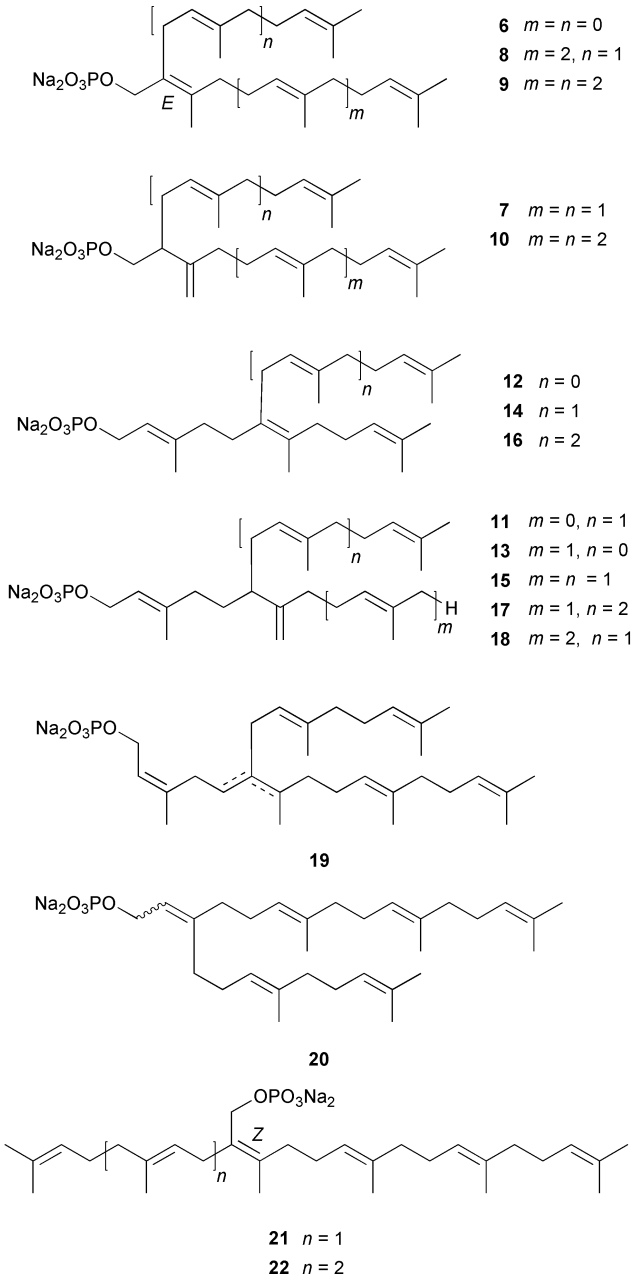

Fig. 2 Structures of synthesized 2- and 6-(poly)prenyl-substituted polyprenyl phosphates **6**–**22**.

acetic acid. pH 7.0: Na_2HPO_4–NaH_2PO_4; pH 7.86: Tris · HCl pH 8.5 and 8.85: borate). Vesicles were observed to grow from the edges of the solid and to detach after establishing their optimal size. Unilamellar and multilamellar vesicles and tubules of various shapes and sizes ranging from 0.2 to 15 μm were observed. The vesicles moved at speeds of 0.15–345 nm s^{-1}. The membranes appear to be thick because of the diffraction-limited resolution of the optical system (interference contrast).

2.2 Metal shadowing cryo-transmission electron microscopy

A typical procedure for the preparation and observation of vesicles was as follows. A phosphate (5 mg) was dissolved in 1 ml of 2 : 1 (v/v) chloroform–methanol. After evaporation of the solvents, the film was dried under vacuum (*ca.* 0.1 Torr) overnight. The lipidic film was then hydrated by addition of 1 ml of a 100 μM sodium acetate–acetic acid buffer (pH 4.5) and the vesicular suspension was sonicated for 2 min at room temperature. 700 Mesh copper grids were dipped into the lipid stock solution (5 mg ml^{-1}) and plunged into liquid ethane cooled with liquid nitrogen. Obtained at the temperature of −100 °C and under high vacuum (pressure: *ca.* 10^{-8} Torr), the digital prints of the micrometrically cut liposome preparation result from a double metallic deposit of Pt/C first (incidence angle 45°; thickness 0.6–1.0 nm) and, thereafter, of C (incidence angle 90°; thickness 6–10 nm). Grids were finally mounted under liquid nitrogen in a Gatan 626 Cryoholder, transferred to the electron microscope and observed at −170 °C. Observations were made in a CM 12 Philips cryo-transmission electron microscope operating at 100 kV. The microscope was equipped with an additional anti-contamination device. Images were not taken under low-dose conditions, as pure lipid solutions are not as sensitive to beam irradiation as proteins. Images were recorded on Kodak SO 163 film and developed under standard conditions.

2.3 Conformational analysis

The conformational analysis of **26**–**33** was performed using the CONFLEX program on a CAChe™ system. CAChe™ is a registered trademark of Oxford Molecular Inc.

2.4 NMR spectroscopy

^1H NMR spectra were recorded on a JEOL GSX-270 (270 MHz) or GSX-400 (400 MHz) spectrometer with $CDCl_3$ as

the solvent and tetramethylsilane as an internal standard. *J* values are given in Hz. ^{13}C NMR spectra were recorded on the spectrometers operating at 67.8 or 100.4 MHz with $CDCl_3$ as the solvent and internal standard (δ 77.00). A spectral width of 5 kHz using 33 K data points was applied to the ^{13}C measurements of carbon–carbon vicinal spin coupling constants. The measurements of spin–lattice relaxation times T_1 were performed using proton-decoupled ^{13}C spectra by the Fourier transform technique on the spectrometers and a pulse sequence (π–τ–Π) at 25 °C. ^{31}P NMR spectra with complete proton decoupling were recorded on the JEOL GSX-270 spectrometer operating at 109.4 MHz in $CDCl_3$ (external standard: phosphoric acid in D_2O). Mass spectra (EI, 70 eV and negative FAB) were obtained on a JEOL JMS-700 mass spectrometer. Accurate mass measurements were made on the mass spectrometer.

2.5 Syntheses

Triethyl phosphonoacetate-1-^{13}C and triethyl phosphonoacetate-2-^{13}C were purchased from Aldrich. Precoated Merck Kieselgel 60 F254 and Wakogel C-300 were used for thin layer chromatography (TLC) and flash column chromatography, respectively. Synthesis of ^{13}C-labeled compounds **44** and **54** was performed according to Schemes 1 and 2.

Disodium (2*E*)-3,7-dimethyl-2-(3-methyl-2-butenyl)-2,6-octadienyl phosphate 6. Oil. ^1H NMR δ 5.08 (1H, m, CH=), 5.01 (1H, t, *J* 6.4, CH=), 4.31 (2H, d, *J* 5.0, 1-H), 2.80 (2H, d, *J* 6.4, 1′-H), 1.99 (4H, m, 2 × CH_2CH=), 1.71 (3H, s, Me), 1.66 (3H, s, Me), 1.62 (3H, s, Me) and 1.58 (3H, s, Me). ^{13}C NMR δ 135.42, 131.26, 129.19, 124.55, 123.30, 64.86, 34.90, 29.74, 29.13, 26.83, 25.69, 18.03, 17.84 and 17.59. ^{31}P NMR δ 5.13 (s). Negative FAB-MS (glycerol): *m/z* 301 [M − (2 × Na^+) + H^+, 100%]. Found: *m/z* 301.1596 [M − (2 × Na^+) + H^+]. Calc. for $C_{15}H_{26}O_4P$: 301.1568.

2-[(*E*)-1,5-Dimethyl-4-hexenylidene]-(4*E*,8*E*)-5,9,13-trimethyl-4,8,12-tetradecatrien-1-ol 56. Oil. IR (neat) 3327 and 997 cm^{-1}. ^1H NMR δ 5.09 (4H, m, 4 × CH=), 4.09 (2H, s, *J* 4.9, 1-H), 2.87 (2H, d, *J* 7.3, 1′-H), 2.08 (12H, m, 6 × CH_2CH=), 1.76 (3H, s, Me), 1.68 (9H, s, 3 × Me), 1.61 (3H, s, Me), 1.59 (6H, s, 2 × Me) and 1.15 (1H, br t, *J* 4.9, OH). MS (EI) *m/z* 358 (M^+, 14%), 340 (M^+–H_2O, 24), 297 (28), 271 (23), 221 (21), 203 (71), 161 (52), 147 (67), 81 (66) and 69 (100). Found: *m/z* 358.3205 (M^+). Calc. for $C_{25}H_{42}O$: 358.3235.

2-[(*E*)-1,5-Dimethyl-4-hexenylidene]-(4*E*)-5,9-dimethyl-4,8-decadien-1-ol 57. Oil. IR (neat) 3329 and 998 cm^{-1}. ^1H NMR δ 5.11–5.02 (3H, m, 3 × CH=), 4.08 (2H, s, *J* 5.0, 1-H), 2.85 (2H, d, *J* 7.3, 1′-H), 2.06 (8H, m, 4 × CH_2CH=), 1.75 (3H, s, Me), 1.67 (9H, s, 3 × Me), 1.59 (3H, s, Me), 1.58 (3H, s, Me) and 1.24 (1H, br s, OH). MS (EI) *m/z* 290 (M^+, 15%), 272 (M^+–H_2O, 11), 259 (M^+–CH_2OH, 16), 229 (18), 221 (25), 203 (65), 161 (34), 147 (63), 109 (55), 81 (49) and 69 (100). Found: *m/z* 290.2645 (M^+). Calc. for $C_{20}H_{34}O$: 290.2610.

6-[(*Z*)-1,5-Dimethyl-4-hexenylidene]-(2*E*,8*E*)-3,9,13-trimethyl-2,8,12-tetradecatrien-1-ol 60. Oil. ^1H NMR δ 5.41 (1H, t-like, *J* 6.9, 2-H), 5.11 (2H, m, 2 × CH=), 5.02 (1H, t-like, *J* 7.5, CH=), 4.14 (2H, d, *J* 6.9, 1-H), 2.73 (2H, d, *J* 7.3, 1′-H), 2.04 (12H, m, 6 × CH_2CH=), 1.69 (3H, s, Me), 1.68 (3H, s, Me), 1.67 (3H, s, Me), 1.66 (6H, s, 2 × Me), 1.60 (3H, s, Me), 1.59 (3H, s, Me) and 1.18 (1H, br s, OH). MS (EI) *m/z* 358 (M^+, 24%), 340 (M^+–H_2O), 289 (58), 271 (34), 203 (56), 189 (34), 161 (38), 147 (57), 109 (62), 93 (58), 81 (59) and 69 (100). Found: *m/z* 358.3198 (M^+). Calc. for $C_{25}H_{42}O$: 358.3235.

Disodium 6-[(*Z*)-1,5-Dimethyl-4-hexenylidene]-(2*E*,8*E*)-3,9,13-Trimethyl-2,8,12-tetradecatrienyl phosphate 14. Oil. ^1H NMR δ 5.35 (1H, m, 2-H), 5.03 (3H, m, 3 × CH=), 4.33 (2H, m, 1-H), 2.67 (2H, d, *J* 5.3, 1′-H), 1.98 (12H, m, 6 × CH_2CH=), 1.66 (3H, s, Me), 1.64 (6H, s, 2 × Me), 1.61 (6H, s, 2 × Me), 1.58 (3H, s, Me) and 1.56 (3H, s, Me) ^{13}C NMR δ 140.61, 134.40, 131.90, 131.00, 128.98, 124.55, 124.28, 123.59, 120.71, 62.08, 39.88, 38.64, 34.72, 31.60, 30.88, 27.28, 26.82, 25.76, 18.12, 17.74 and 16.20. ^{31}P NMR δ 3.47 (br s). Negative FAB-MS (glycerol) *m/z* 437 [M − (2 × Na^+) + H^+, 100%)]. Found: *m/z* 437.2793 [M − (2 × Na^+) + H^+]. Calc. for $C_{25}H_{42}O_4P$: 437.2820.

6-[(*Z*)-1,5-Dimethyl-4-hexenylidene]-(2*E*,8*E*,12*E*)-3,9,13,17-tetramethyl-2,8,12,16-octadecatetraen-1-ol 61. Oil. ^1H NMR δ 5.41 (1H, t, *J* 6.9, 2-H), 5.10 (3H, m, 3 × CH=), 5.03 (1H, t-like, *J* 7.3, CH=), 4.15 (2H, d, *J* 6.0, 1-H), 2.73 (2H, d, *J* 7.3, 1′-H), 2.04 (16H, m, 8 × CH_2CH=), 1.69 (3H, s, Me), 1.68 (6H, s, 2 × Me), 1.65 (6H, s, 2 × Me) and 1.60 (9H, s, 3 × Me). ^{13}C NMR δ 140.17, 134.81, 134.71, 131.85, 131.20, 131.13, 129.06, 124.42, 124.30, 124.08, 123.49, 123.00, 59.43, 39.87, 39.77, 38.41, 34.60, 31.16, 30.82, 27.26, 26.83, 26.71, 25.78, 25.75, 18.19, 17.75, 17.70, 16.42, 16.24 and 16.09. MS (EI) *m/z* 426 (M^+, 5%), 408 (M^+ − H_2O, 4) , 339 (9), 271 (12), 203 (22), 147 (22), 109 (26), 81 (42) and 69 (100). Found: *m/z* 426.3906 (M^+). Calc. for $C_{30}H_{50}O$: 426.3862.

Disodium 6-[(*Z*)-1,5-dimethyl-4-hexenylidene]-(2*E*,8*E*,12*E*)-3,9,13,17-tetramethyl-2,8,12,16-octadeca tetraenyl phosphate 16. Oil. ^1H NMR δ 5.37 (1H, br t, *J* 6.3, 2-H), 5.08 (2H, m, 2 × CH=), 4.98 (2H, m, 2 × CH=), 4.35 (2H, br s, 1-H), 2.68 (2H, d, *J* 4.0, 1′-H), 1.99 (16H, m, 8 × CH_2CH=), 1.66 (6H, s, 2 × Me), 1.65 (3H, s, Me), 1.62 (3H, s, Me), 1.61 (3H, s, Me), 1.58 (3H, s, 2 × Me) and 1.57 (3H, s, Me). ^{13}C NMR δ 140.96, 134.82, 134.57, 131.98, 131.10, 129.15, 124.63, 124.43, 124.23, 123.60, 120.65, 62.17, 39.86, 39.73, 38.56, 34.64, 31.50, 30.77, 27.20, 26.78, 25.67, 18.02, 17.64, 17.59, 16.21, 16.13 and 15.97. ^{31}P NMR δ 4.29 (br s).Negative FAB-MS (glycerol) *m/z* 505 [M − (2 × Na^+) + H^+, 77%] and 183 (100). Found: *m/z* 505.3425 [M − (2 × Na^+) + H^+]. Calc. for $C_{30}H_{50}O_4P$: 505.3447.

Ethyl [2-^{13}C]-(2*E*/*Z*,6*E*)-3,7,11-trimethyl-2,6,10-dodecatrienoates 35. A solution of triethyl phosphonoacetate-2-^{13}C (99 atom% ^{13}C, 90 mg, 0.40 mmol) in dry THF (0.5 ml) cooled to 0 °C was added dropwise to a suspension of sodium hydride (60% in mineral oil, 32 mg, 0.80 mmol) in dry THF (2.0 ml) under nitrogen. The mixture was stirred at room temperature for 1 h and cooled to 0 °C. Geranylacetone **34** (155 mg, 0.80 mmol) was added dropwise and the mixture stirred at this temperature for 3 h. Water was added and the aqueous solution extracted three times with diethyl ether. The combined ether solutions were washed with water and saturated brine, and dried over anhydrous sodium sulfate. Evaporation gave a crude product which was chromatographed on silica gel (5.3 g; hexane–diethyl ether, 40 : 1) to give the α,β-unsaturated ester **35** as a mixture of diastereomers (115 mg, 89%, 2*E* : 2*Z* = 4.4 : 1) as an oil. **35*E***: ^1H NMR δ 5.66 (1H, d, $^1J_{CH}$ 159, ^{13}CH=), 5.08 (2H, m, 2 × =CH), 4.14 (2H, q, *J* 7.1, CH_2CH$_3$), 2.16 (7H, m, Me and 2 × =CCH_2), 2.00 (4H, m, 2 × =CCH_2), 1.68 (3H, s, Me), 1.60 (6H, s, 2 × Me) and 1.28 (3H, t, *J* 7.1, CH$_2$CH_3); ^{13}C NMR δ 115.90 (s, ^{13}C-enriched =CH); MS (EI) *m/z* 265 (M^+, 20%), 220 (M^+ − OEt, 28), 129 (93) and 69 (100); Found *m/z* 265.2079 (M^+); Calc. for $C_{16}{}^{13}CH_{28}O_2$ 265.2123. **35*Z***: ^1H NMR δ 5.65 (1H, dq, *J* 159, 1.2, ^{13}CHCO$_2$), 5.09 (2H, m, 2 × =CH), 4.14 (2H, q, *J* 7.2, CH_2CH$_3$), 2.65 (2H, td, *J* 7.8, 4.5, =CCH_2), 2.16 (2H, m, =CCH_2), 2.06 (2H, q, *J* 7.3, =CCH_2), 1.98 (2H, t, *J* 7.3, =CCH_2), 1.89 (3H, dd, *J* 6.1, 1.2, Me), 1.68 (3H, s, Me), 1.60

(6H, s, 2 × Me) and 1.27 (3H, t, *J* 7.3, CH_2CH_3); ^{13}C NMR δ 116.23 (s, ^{13}C-enriched =CH).

[2-^{13}C]-(2*E*,6*E*)-3,7,11-Trimethyl-2,6,10-dodecatrien-1-ol 36. To a solution of the ester **35** (*E* major; 105 mg, 0.40 mmol) in anhydrous diethyl ether (9.9 ml) was added a solution of diisobutylaluminium hydride in hexane (0.95 M; 1.3 ml, 1.2 mmol) at 0 °C and the solution stirred at this temperature for 50 min. An aqueous solution of sodium hydroxide (10%) and diethyl ether were added. The organic layer was washed successively with aqueous NaOH (10%), water (until neutral) and brine, and dried over anhydrous sodium sulfate. Chromatography on silica gel (10 g; hexane–diethyl ether, 4 : 1) gave the alcohol **36** (82 mg, 92%) as an oil.

[2-^{13}C]-(2*E*,6*E*)-1-Bromo-3,7,11-trimethyl-2,6,10-dodecatriene 37. To a solution of the alcohol **36** (82 mg, 0.37 mmol) in anhydrous diethyl ether (1.2 ml) was added pyridine (9.8 mg, 0.12 mmol) under nitrogen. The mixture was cooled to 0 °C and phosphorus tribromide (33 mg, 0.12 mmol) added dropwise. After 20 min, saturated aqueous sodium hydrogencarbonate was added, and the crude product extracted with diethyl ether. The organic layer was washed with saturated aqueous sodium hydrogencarbonate, water and brine, and the solvent evaporated to give the bromide **37** (88 mg, 84% yield) as a pale yellow oil. The bromide (*E* major) was used for the following reaction without further purification.

Ethyl [1-^{13}C]-(2*E*/*Z*,6*E*)-3,7,11-Trimethyl-2,6,10-dodecatrienoates 38. Following the procedures described for the preparation of **35**, the compounds were prepared from triethyl phosphonoacetate-1-^{13}C (99 atom% ^{13}C; 90 mg, 0.4 mmol) and geranylacetone **34** (116 mg, 0.8 mmol) in 57% yield and in a ratio of $E : Z = 7 : 1$. **38*E***: ^{13}C NMR δ 166.90 (s, ^{13}C-enriched C=O). **38*Z***: ^{13}C NMR ($CDCl_3$) δ 166.35 (s, ^{13}C-enriched C=O).

[1-^{13}C]-(2*E*,6*E*)-3,7,11-Trimethyl-2,6,10-dodecatrien-1-ol 39. Following the procedures described for the preparation of **36**, the compound (*E* major) was prepared from **38** in 86% yield.

***N*-{[1-^{13}C]-(2*E*,6*E*)-3,7,11-Trimethyl-2,6,10-dodecatrienylidene}cyclohexylamine 41.** A mixture of activated MnO_2 (332 mg) and the alcohol **39** (41 mg, 0.18 mmol) in hexane (2.3 ml) was stirred at room temperature for 3 h. After filtration, the solvent was evaporated to give the corresponding aldehyde (30 mg, 73% yield) as a pale yellow oil. To a solution of the aldehyde (41 mg, 0.13 mmol) in benzene (0.8 ml) cooled to 0 °C were added cyclohexylamine (28 mg, 0.28 mmol) and potassium carbonate (6 mg, 0.04 mmol). The mixture was stirred at 0 °C for 1 h and then at room temperature for 1 h. After filtration the solvent was evaporated to give quantitatively the imine **41**.

[1, 4-$^{13}C_2$]-(4*E*,8*E*)-5,9,13-Trimethyl-2-[(*E*)-1,5,9-trimethyl-4,8-decadienylidene]-4,8,12-tetradecatrienal 42 and [1,4-$^{13}C_2$]-(4*E*,8*E*)-5,9,13-trimethyl-2-[(*Z*)-1,5,9,13-tetramethyl-4,8,12-tetradecatrienylidene]-4,8,12-tetradecatrienal 43. Following the procedures reported previously,[9a] the imine **41** (0.13 mmol) was treated with lithium diisopropylamide and then with the bromide **37** (88 mg, 0.31 mmol) to give **42** (5.6 mg, 10% yield; including γ-substituted isomer) and **43** (43 mg, 76% yield). Acid-catalyzed isomerization of **43** gave **42**.[9c]

42: ^1H NMR δ 10.15 (1H, d J_{CH} 172, ^{13}CH=O), 5.08 (4H, m, 4 × CH=), 4.92 (1H, dt, J_{CH} 153, 5.8, ^{13}CH=), 2.99 (2H, d, *J* 4.6, 1′-H), 2.28 (2H, m, CH_2), 2.19 (2H, m, CH_2), 2.19 (3H, s, Me), 2.05 (6H, m, 3 × CH_2), 1.97 (6H, m, 3 × CH_2), 1.68 (9H, s, 3 × Me), 1.61 (3H, s, Me), 1.60 (6H, s, 2 × Me) and 1.57 (3H, s, Me); ^1H decoupled ^{13}C NMR δ 191.32 (d, $^3J_{CC}$ 0.62, ^{13}C-enriched CH=O) and 122.21 (d, $^3J_{CC}$ 0.62, ^{13}C-enriched CH=); ^1H non-decoupled ^{13}C NMR δ 191.32 (d, J_{CH} 172, ^{13}C-enriched CH=O) and 122.21 (dt, J_{CH} 153, 4.6, ^{13}C-enriched CH=); MS (EI) *m*/*z* 426 (M^+, 2), 408 ($M^+ - H_2O$, 1), 81 (43) and 69 (100); Found *m*/*z* 426.3813; Calc. for $C_{28}{}^{13}C_2H_{48}O$ 426.3772.

43: ^1H NMR δ 10.04 (1H, d J_{CH} 171, ^{13}CH=O), 5.09 (4H, m, 4 × CH=), 5.07 (1H, d, J_{CH} 154, ^{13}CH=), 2.98 (2H, m, 1′-H), 2.60 (2H, t, *J* 7.5, CH_2), 2.29 (2H, q, *J* 7.5, CH_2), 2.05 (12H, m, 6 × CH_2), 1.97 (3H, s, Me), 1.68 (9H, s, 3 × Me), 1.60 (9H, s, 3 × Me) and 1.58 (3H, s, Me); ^1H decoupled ^{13}C NMR δ 190.37 (d, $^3J_{CC}$ 0.61, ^{13}C-enriched CH=O) and 121.62 (d, $^3J_{CC}$ 0.61, ^{13}C-enriched CH=); ^1H non-decoupled ^{13}C NMR δ 190.37 (d, J_{CH} 171, ^{13}C-enriched CH=O) and 121.62 (dt, J_{CH} 154, 4.6, ^{13}C-enriched CH=); MS (EI) *m*/*z* 426 (M^+, 2), 408 ($M^+ - H_2O$, 1), 139 (14), 109 (11), 81 (21) and 69 (100); Found *m*/*z* 426.3797; Calc. for $C_{28}{}^{13}C_2H_{48}O$ 426.3772.

[1, 4-$^{13}C_2$]-(4*E*,8*E*)-5,9,13-Trimethyl-2-[(*E*)-1,5,9-trimethyl-4,8-decadienylidene]-4,8,12-tetradecatrien-1-ol 44 and [1, 4-$^{13}C_2$]-(4*E*,8*E*)-5,9,13-trimethyl-2-[(*Z*)-1,5,9,13-tetramethyl-4,8,12-tetradecatrienylidene]-4,8,12-tetradecatrien-1-ol 45. Following the procedures described previously,[9a] the aldehydes **42** and **43** were reduced with diisobutylaluminium hydride to give the alcohols **44** and **45**, respectively.

44: ^1H NMR δ 5.11 (2H, m, 2 × CH=), 5.09 (2H, m, 2 × CH=), 5.07 (1H, dt, $^1J_{CH}$ 152, 6.8, ^{13}CH=), 4.09 (2H, d, $^1J_{CH}$ 142, $^{13}CH_2OH$), 2.88 (2H, dd, $^2J_{CH}$ 5.6, $^3J_{HH}$ 6.8, 1′-CH_2), 2.09 (4H, m, 2 × CH_2), 2.08 (4H, m, 2 × CH_2), 2.04 (4H, m, 2 × CH_2), 1.99 (4H, m, 2 × CH_2), 1.77 (3H, s, Me), 1.68 (9H, s, 3 × Me) and 1.60 (12H, s, 4 × Me); ^1H decoupled ^{13}C NMR δ 122.92 (d, $^3J_{CC}$ 0.77, ^{13}C-enriched CH=) and 62.51 (d, $^3J_{CC}$ 0.77, ^{13}C-enriched CH_2OH); ^1H non-decoupled ^{13}C NMR δ 122.92 (d, $^1J_{CH}$ 152, ^{13}C-enriched CH=) and 62.51 (d, $^1J_{CH}$ 142, ^{13}C-enriched CH_2OH); MS (EI) *m*/*z* 428 (M^+, 24), 410 ($M^+ - H_2O$, 13), 273 (64), 149 (45), 137 (59), 122 (53), 109 (60), 81 (85) and 69 (100); Found: *m*/*z* 428.3948; Calc. for $C_{28}{}^{13}C_2H_{50}O$ 428.3929.

45: ^1H NMR δ 5.15 (1H, t-like, *J* 7.6, CH=), 5.09 (3H, m, 3 × CH=), 5.07 (1H, dt, $^1J_{CH}$ 151, 6.6, ^{13}CH=), 4.06 (2H, dd, $^1J_{CH}$ 142, $^3J_{HH}$ 5.3, $^{13}CH_2OH$), 2.86 (2H, dd, $^2J_{CH}$ 5.6, $^3J_{HH}$ 6.6, 1′-CH_2), 2.04 (16H, m, 8 × CH_2), 1.73 (3H, s, Me), 1.68 (9H, s, 3 × Me) and 1.60 (12H, s, 4 × Me); ^1H decoupled ^{13}C NMR δ 122.53 (d, $^3J_{CC}$ 0.70, ^{13}C-enriched CH=) and 61.99 (d, $^3J_{CC}$ 0.70, ^{13}C-enriched CH_2OH); ^1H non-decoupled ^{13}C NMR δ 122.53 (d, $^1J_{CH}$ 151, ^{13}C-enriched CH=) and 62.00 (d, $^1J_{CH}$ 142, ^{13}C-enriched CH_2OH); MS (EI) *m*/*z* 428 (M^+, 11), 410 ($M^+ - H_2O$, 5) and 69 (100); Found *m*/*z* 428.3929; Calc. for $C_{28}{}^{13}C_2H_{50}O$ 426.3929.

Ethyl (4*E*)-2-{[1-^{13}C]acetyl}-5,9-dimethyl-4,8-decadienoate 47. To a suspension of sodium hydride (60% in mineral oil; 51 mg, 1.27 mmol) in anhydrous THF (9.3 ml) cooled to 0 °C was added a solution of ethyl [3-^{13}C]acetoacetate (99 atom% ^{13}C, 849 mg, 3.91 mmol) in anhydrous THF (1.0 ml) under argon. The mixture was stirred at room temperature for 30 min and then cooled to 0 °C. A solution of geranyl bromide (0.85 g, 3.9 mmol) in anhydrous THF (6 ml) was added and the mixture stirred at room temperature for 3 h. Quenching with water and the usual work-up followed by flash chromatography on silica gel gave **47** (163 mg, 62% yield) as an oil and ethyl (4*E*)-2-([1-^{13}C]acetyl)-2-[(2*E*)-3,7-dimethyl-6-octenyl]-5,9-dimethyl-4,8-decadienoate (oil; 97 mg, 33% yield). Spectral data for **47**: ^1H NMR δ 5.05 (1H, m, CH=), 5.04 (1H, m, CH=), 4.18 (2H, q, *J* 7.0, OCH_2CH_3), 3.44 (1H, dq, $^3J_{HH}$ 7.5, $^2J_{CH}$ 5.8, ^{13}C(=O)CH), 2.55 (2H, m, CH_2), 2.22 (3H, d, $^2J_{CH}$ 6.1, ^{13}C(=O)Me), 2.04 (2H, q, *J* 7.3, CH_2), 1.97 (2H, t, *J* 7.3, CH_2), 1.67 (3H, s, Me), 1.63 (3H, s, Me), 1.59 (3H, s, Me) and 1.27 (3H, t, *J* 7.0, Me); ^{13}C NMR δ 203.18 (s, ^{13}C-enriched C=O).

[2-^{13}C]-(5*E*)-6,10-Dimethyl-5,9-undecadien-2-one 48. To a solution of the β-keto ester **47** (163 mg, 0.61 mmol) in ethanol (9 ml) was added an aqueous solution of sodium hydroxide (1.6 M; 16 ml). The mixture was stirred at 50 °C for 2 h and then acidified with acetic acid. After evaporation of the solvent the residue was extracted with diethyl ether. The crude product was chromatographed on silica gel (30 g; hexane–ethyl acetate, 20 : 1) to give the methyl ketone **48** (96 mg, 81%), an oil. ^{1}H NMR δ 5.08 (2H, m, 2 × CH=), 2.46 (2H, dt, $^3J_{HH}$ 7.3, $^2J_{CH}$ 5.5, ^{13}C(=O)CH$_2$), 2.27 (2H, m, CH$_2$), 2.14 (3H, d, $^2J_{CH}$ 5.8, ^{13}C(=O)Me), 2.05 (2H, m, CH$_2$), 1.97 (2H, m, CH$_2$), 1.68 (3H, s, Me), 1.61 (3H, s, Me) and 1.60 (3H, s, Me). ^{13}C NMR δ 208.94 (s, ^{13}C-enriched C=O).

Ethyl [3-^{13}C]-(2*E*,6*E*)-3,7,11-Trimethyl-2,6,10-dodecatrienoate 49. Following the procedures described for the preparation of **35**, the α,β-unsaturated ester **49** was prepared from triethyl phosphonoacetate (1.56 g, 6.98 mmol) and the ketone **48** (136 mg, 0.70 mmol) as a mixture of *E* and *Z* diastereomers in 75% yield.

[3-^{13}C]-(2*E*,6*E*)-3,7,11-Trimethyl-2,6,10-dodecatrien-1-ol 50. Following the procedures for the preparation of **36**, the α,β-unsaturated ester **49** was reduced with diisobutylaluminium hydride to give **50** in 93% yield together with the corresponding 2,3-epoxy alcohol (6%). Spectral data of **50**: ^{1}H NMR δ 5.42 (1H, t-like, *J* 7.1, 2-H), 5.11 (1H, m, CH=), 5.09 (1H, m, CH=), 4.16 (2H, d, *J* 7.1, 1-CH$_2$), 2.05 (8H, m, 4 × CH$_2$), 1.70 (3H, d, $^2J_{CH}$, 4.9, Me), 1.68 (3H, s, Me) and 1.60 (3H, s, Me); ^{13}C NMR δ 139.78 (s, ^{13}C-enriched C=O).

[3-^{13}C]-(2*E*,6*E*)-1-Bromo-3,7,11-trimethyl-2,6,10-dodecatriene 51. Following the procedures described for the preparation of **37**, the alcohol **50** was treated with phosphorus tribromide to give the bromide **51** in 78% yield.

(2*E*,6*E*)-3,7,11-Trimethyl-2,6,10-dodecatrienal 52. Following the procedures described for the preparation of the imine **41**, the alcohol **36** was oxidized with activated MnO_2 to give **52** in 92% yield as an oil, ^{1}H NMR δ 10.00 (1H, dd, $^2J_{CH}$ 24.4, $^3J_{HH}$ 8.1, CH=O), 5.88 (1H, dd, $^1J_{CH}$ 158, $^3J_{HH}$ 8.1, CH=), 5.07 (2H, m, 2 × CH=), 2.23 (4H, m, 2 × CH$_2$), 2.17 (3H, dd, $^3J_{CH}$ 4.3, $^4J_{HH}$ 1.2 H, Me), 2.04 (4H, m, 2 × CH$_2$), 1.68 (3H, s, Me) and 1.60 (6H, s, 2 × Me). ^{13}C NMR δ 127.32 (s, ^{13}C-enriched C-2). MS (EI) *m*/*z* 221 (M$^+$, 27%), 203 (M$^+$ − H$_2$O, 15), 178 (27), 150 (23), 136 (67), 123 (49), 109 (51), 85 (92), 81 (63) and 69 (100). Found: *m*/*z* 221.1832 (M$^+$). Calc. for C$_{14}$^{13}CH$_{24}$O: 221.1861.

[2,5-^{13}C$_2$]-(4*E*,8*E*)-5,9,13-Trimethyl-2-[(*E*)-1,5,9-trimethyl-4,8-decadienylidene]-4,8,12-tetradecatrien-1-ol 54 and [2,5-^{13}C$_2$]-(4*E*,8*E*)-5,9,13-trimethyl-2-[(*Z*)-1,5,9,13-tetramethyl-4,8,12-tetradecatrienylidene]-4,8,12-tetradecatrien-1-ol 55. The aldehyde **52** was then transformed into **54** and **55** following the procedures reported above. It was treated with cyclohexylamine to give **53**. Allylation of the carbanion of **53** with the bromide **51**, followed by acid-catalyzed hydrolysis, gave (2*E*)- and (2*Z*)-2-farnesylfarnesals. Acid-catalyzed isomerization of the (2*Z*)-aldehyde gave the (2*E*) isomer in pure form. Reduction of the (2*E*)- and (2*Z*)-2-farnesylfarnesals with diisobutylaluminium hydride gave **54** and **55**, respectively.

54: ^{1}H NMR δ 5.11 (2H, m, 2 × CH=), 5.09 (2H, m, 2 × CH=), 5.07 (1H, m, CH=), 4.10 (2H, d, $^2J_{CH}$ 3.3, 1-H), 2.88 (2H, dd, $^3J_{HH}$ 6.3, $^2J_{CH}$ 5.9, 1′-H), 2.09–1.99 (16H, m, 8 × CH$_2$), 1.77 (3H, d, $^3J_{CH}$ 4.9, Me), 1.68 (9H, s, 3 × Me) and 1.60 (12H, s, 4 × Me); ^{1}H-decoupled ^{13}C NMR δ 136.10 (d, $^3J_{CC}$ 2.8, ^{13}C-enriched 3′-C) and 131.78 (d, $^3J_{CC}$ 2.8, ^{13}C-enriched 2-C); MS (EI) *m*/*z* 428 (M$^+$, 11%), 410 (M$^+$ − H$_2$O, 6), 273 (41), 149 (35), 137 (44), 123(45), 109 (56), 95 (60), 81 (86) and 69 (100); Found *m*/*z* 428.3959 (M$^+$); Calc. for C$_{28}$^{13}C$_2$H$_{50}$O 428.3929.

55: ^{1}H NMR δ 5.11 (2H, m, 2 × CH=), 5.09 (2H, m, 2 × CH=), 5.07 (1H, m, CH=), 4.07 (2H, d, $^3J_{HH}$ 5.3, $^2J_{CH}$ 3.3, 1-H), 2.85 (2H, dd, $^3J_{HH}$ 6.3, $^2J_{CH}$ 5.9, 1′-H), 2.04–1.97 (16H, m, 8 × CH$_2$), 1.72 (3H, d, $^3J_{CH}$ 5.0, Me), 1.68 (9H, s, 3 × Me) and 1.60 (12H, s, 4 × Me); ^{1}H-decoupled ^{13}C NMR δ 135.73 (d, $^3J_{CC}$ 2.8, ^{13}C-enriched 3′-C) and 132.26 (d, $^3J_{CC}$ 2.8, ^{13}C-enriched 2-C); MS (EI) *m*/*z* 428 (M$^+$, 32%), 410 (M$^+$ − H$_2$O, 12), 273 (39), 137 (40), 123 (37), 109 (36), 81 (58) and 69 (100); Found *m*/*z* 428.3929 (M$^+$); Calc. for C$_{28}$^{13}C$_2$H$_{50}$O 428.3929.

3 Results and discussion

3.1 Vesicle formation

The spontaneous formation of vesicles (liposomes) depends on the relative sizes of the hydrophilic and hydrophobic parts in the molecule. For bilayer-forming lipids the critical packing parameter v/a_0l_c (a_0 = the optimal area per molecule at the lipid–water interface; l_c = chain length; v = hydrocarbon volume) must lie between 1/2 and 1.[10] The lipids with two chains adopting cylindrical shapes would be accommodated in the bilayer phase. The surface area a_0 depends on the net charge of the polar region. Charge repulsion increases the effective area per molecule in the polar region and therefore the effective area of the phosphate group increases in the order : diacid < monoanion < dianion. In order to reveal the relationships between the pH values of buffers and the sizes of lipophilic polyprenyl chains in the spontaneous vesicle formation of the phosphates **6**–**20**, we examined the vesicle formation in buffers of pH range 3.1–8.85, following the procedures described in the Experimental section. Vesicle formation was observed by differential interference contrast microscopy at 25.0 °C. Unilamellar vesicles of diameter larger than 0.2 μm were observed, besides multilamellar structures and tubules. A summary of the results is shown in Table 1, from which we can draw the following conclusions.

2-Prenylgeranyl phosphate **6** formed vesicles spontaneously in buffers of pH 3.1, 4.0 and 4.5. Fig. 3 shows an optical micrograph of the vesicles of **6** prepared at pH 3.1. In contrast, it has been reported that the single-chain farnesyl phosphate **1** (n = 1, C$_{15}$) forms only very small vesicles which were detected by electron microscopy, but no giant vesicle was seen by optical microscopy.[2c] Furthermore, prenylgeranyl phosphate **2**, with one C$_5$ and one C$_{10}$ chain (m = 0, n = 1), has been shown to give a clear solution in water.[2a,b] Potentiometric measurements with phytyl phosphate **24** and related compounds have shown their dissociation constants to be: pK_{a1} 3.2–3.3 and pK_{a2} 6.6–6.7.[2c] Under acidic conditions, the phosphate **6** would be present as diacid or monoanionic

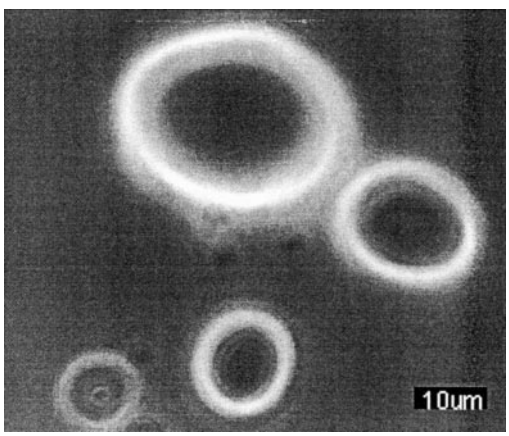

Fig. 3 Phase contrast microscope images of the giant vesicles of phosphate **6** at pH 3.1.

Table 1 Spontaneous vesicle formation of sodium polyprenyl phosphates **6**–**20** at various pH values[a]

Phosphate	Number of C atoms (Main and side chains)	pH Value of buffer[b]						
		3.1	4.0	4.5	7.0	7.86	8.5	8.85
6	15(10 + 5)	+	+	+	−		−	
7	25(15 + 10)	−	−	−	+	+	+	
8	30(20 + 10)	−			+		+	+
9	35(20 + 15)	−	−	−	−		+	+
10	35(20 + 15)	−	−	−	−		+	+
11	20(10 + 10)	−		+	+	+	+	
12	20(15 + 5)	+		+	+			−
13	20(15 + 5)	−	−	+	+	+		−
14	25(15 + 10)	+			+		+	
15	25(15 + 10)	+			+		+	
16	30(15 + 15)	−		+	+		+	
17	30(15 + 15)			−	+		+	
18	30(20 + 10)							+
19	30(20 + 10)			−	+			+
20	30(20 + 10)	−			−	+	+	+

[a] Observed by differential interference contrast microscopy at 25.0 ± 0.1 °C. [b] pH 3.1 and 4.5; acetate buffer; pH 7.0, phosphate buffer; pH 7.86; Tris · HCl buffer; pH 8.5 and 8.85; borate buffer. +; Vesicle formation; −; no vesicle formation; blank; not tested.

forms, with smaller polar heads than those of the dianion form. In the buffers of pH 7.0 and 8.5 the dianion of phosphate **6** did not form vesicles, due to the higher hydro- : lipophilicity ratio.[10]

The higher isoprenologs **7** and **8**, which possess C_{15} and C_{20} main chains and a C_{10} side chain at C-2, did not form vesicles under acidic conditions, but did so at pH 7.0 and higher. Further increase of the size of the lipophilic polyprenyl chains, as in the case of 2-farnesyl-substituted geranylgeranyl phosphates **9** and **10**, inhibited vesicle formation in the buffers of pH 7.86 and lower: their hydro- : lipo-philicity ratios are inappropriate for vesicle formation. The vesicle formation of the isomeric phosphates **9** and **10** indicates that the double bond positions are indifferent (*vide infra*).

The spherical structure of the vesicles prepared by sonication of phosphate **8** in pH 4.5 acetate buffer (10^{-4} M) was confirmed by metal shadowing cryo-transmission electron microscopy (Fig. 4; the white parts of the images are due to the side-shadowing). The vesicles of **8**, prepared by vortex mixing in pH 7.0 phosphate buffer (10^{-4} M), were also observed by negative staining (3% Ac_2UO_2) transmission electron microscopy (Fig. 5).

In the vesicle formation with 6-(poly)prenyl-substituted polyprenyl phosphates **11**–**19** a similar trend was observed in the relationship between the pH values of buffers and the sizes of the lipophilic polyprenyl chains.

Both the phosphate **11** (disodium 6-isopropenyl-3,9-dimethyl-2,8-decadienyl phosphate) and the slightly larger homolog **13** (disodium 6-isopropyl-3,11-dimethyl-7-methylene-2,10-dodecadienyl phosphate) formed vesicles in the pH range 4.5–8.5 (Fig. 6), but neither in a highly acidic buffer (pH 3.1) nor in a basic buffer (pH 8.85 for **13**).

Both phosphates **14** and **15** formed vesicles in a wide range of pH (3.1–8.5). However, the phosphate **12** and its isomer **13** showed different behaviours in vesicle formation. The former, possessing a prenyl chain attached to the sp^2 carbon atom (C-6), formed vesicles at pH 3.1, but not the latter possessing a prenyl chain at the sp^3 carbon atom (C-6). A similar trend was observed for the isoprenologs **16** and **17** at pH 4.5, *i.e.* the former formed vesicles at this pH but not the latter.

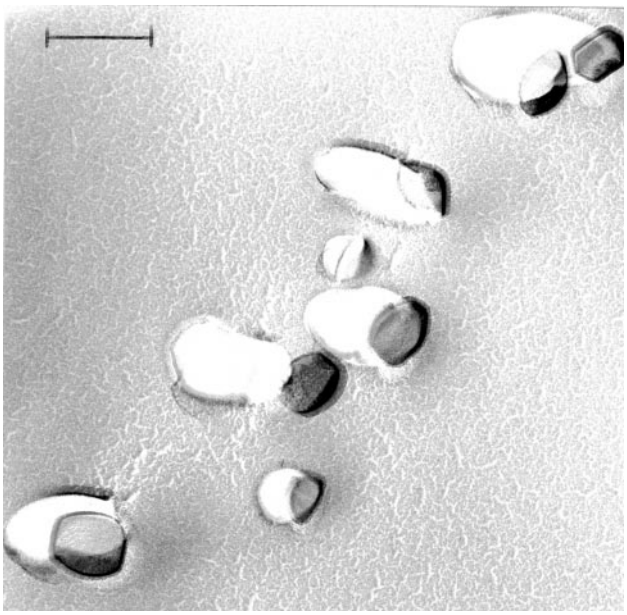

Fig. 4 Cryo-transmission electron microscope shadowed images of the vesicles of phosphate **8** prepared by sonication in pH 4.5 acetate buffer (10^{-4} M). The black part of the images corresponds to the carbon shadowing (90°) and the white to the platinum shadowing (45°). The bar represents 0.5 μm.

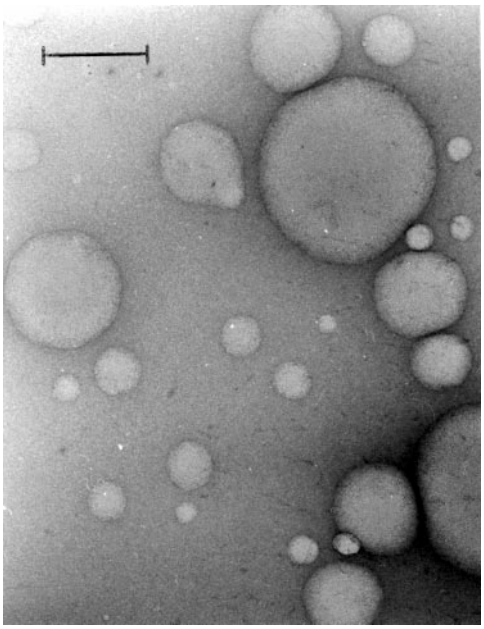

Fig. 5 Negatively stained (3% Ac_2UO_2) electron microscope images of the vesicles of phosphate **8** prepared by vortex mixing in pH 7.0 phosphate buffer (10^{-4} M). The bar represents 0.5 μm.

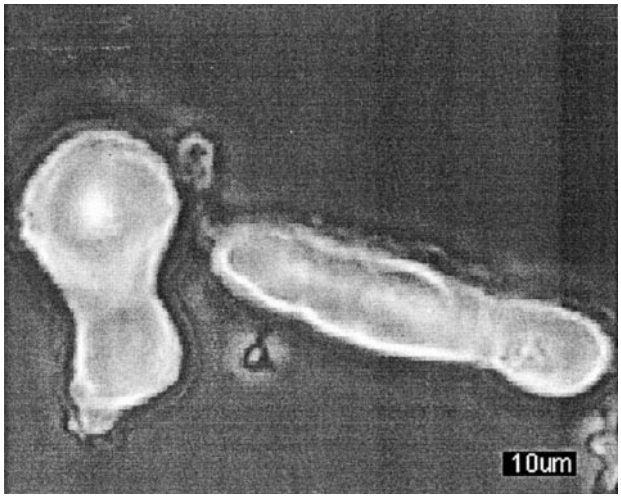

Fig. 6 Phase contrast micrograph of giant vesicles of phosphate **11**.

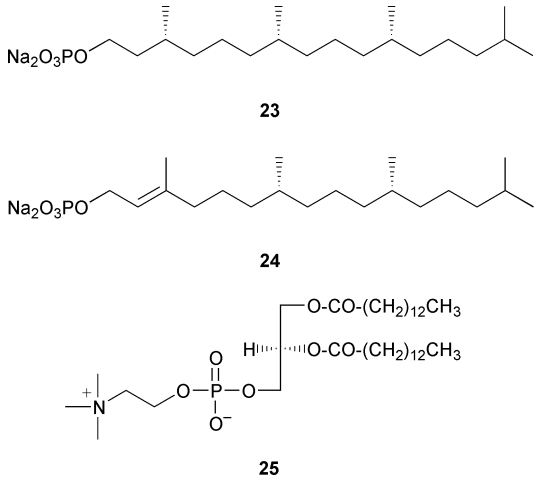

Fig. 7 Structures of **23**, **24** and **25**.

The large lipophilic portion of the phosphate **19** was inappropriate for vesicle formation under acidic conditions and required the larger polar head-group of the dianion to obtain an adequate hydrophilic : lipophilic ratio.

The phosphate **20**, which was derived as a by-product from the synthesis of **8**, but was not a candidate primitive biomembrane constituent,[9a] formed vesicles at pH higher than 7.0.

Thus, Table 1 shows that the 6-polyprenyl-substituted polyprenyl phosphates **11**–**19** form vesicles in a wide range of pH, unlike the 2-polyprenyl-substituted polyprenyl phosphates **6**–**10**. We shall discuss the differences in vesicle formation and their compactness in the following sections.

We also attempted the preparation of vesicles of **21** and **22**, but as predicted for their 2*Z* geometry no vesicle formation was observed by optical microscopy (see: the global minimum conformation in Fig. 12).

3.2 Water permeability of the vesicles

In order to evaluate the rigidity of the vesicles of phosphates **1** ($n = 2$), **11**, **20** and **23**–**25** (Fig. 7), osmotic swelling of the unilamellar vesicles was measured by use of the stopped-flow/light-scattering method at pH 7.86 and at 33 °C.[2b,11] Following the procedures described previously,[2b] the vesicles of these phospates were prepared and we measured their water permeability. The results are summarized in Table 2 together with those previously reported.[2b] The phosphate **20** showed an average first-order rate constant similar to those of 1,2-dimyristoyl-*sn*-glycero-3-phosphocholine (DMPC) **25**[11] and difarnesyl phosphate **2** ($m = n = 2$). It was also observed that, when the chain length increases from C_{15} [**2** ($m = n = 2$)] to C_{20} [**2** ($m = n = 3$)], the water permeability decreases. This could be due to the increase in the attractive cooperative van der Waals forces. Phosphate **11** showed a rate constant similar to those of disodium (7*R*,11*R*)-phytyl phosphate **24** and disodium geranylgeranyl phosphate (**1**, $n = 2$). These unexpected results indicate that the vesicles of the unsaturated polyprenyl phosphates are more impermeable to water, by a factor of 100, than those of the saturated polyprenyl phosphates. However, it has been shown that phosphate **24** does not form stable monolayers in alkaline solutions and phosphate **1** ($n = 2$) does not form monolayers even under acidic conditions.[12] The decomposition of the unstable vesicles during mixing (*ca.* 3 ms) and/or swelling may be the cause of the extremely small rate constant in this case.

Closed vesicles should be capable of holding inside their cavity hydrophilic molecules unable to cross the lipid layer.[2] However, the entrapment of calcein, a hydrophilic dye, in the vesicles of **14** failed, probably because the membranes were unstable and the dye therefore leaked out rapidly through the loosely packed membranes.[13] We abandoned further attempts to measure the permeability of the other phosphates.

3.3 Calculations of intramolecular attractive van der Waals forces

Among the major forces holding the membrane molecules together are van der Waals forces between the hydrocarbon chains of adjacent lipid molecules. The stability of the vesicles mentioned above should also depend on both the rigidity of each unsaturated hydrophobic chain and on the intramolecular attractive van der Waals forces between the chains. It has been shown that unsaturated chains are more mobile in solution than their saturated counterparts.[14] To evaluate the stability of the vesicles of **20**, we estimated the intramolecular attractive van der Waals forces between the two chains **a** and **b** in the alkene **27** and docosane **26**. The latter was chosen as a substitute for the saturated counterpart of **27** (Fig. 8).

Table 2 Shrinkage experiments on vesicles of phosphates **1**, **2**, **11**, **20** and **23**–**25**

Phosphate	d_{av}[a]/nm	SD[b]/nm	k[c]/s^{-1}	SD[b]	Reference
11	86	27	2.0×10^{-2}	0.1×10^{-2}	*d*
20	106	21	39.8	0.8	*d*
23	91	28	3.5	0.1	*d*
24	94	19	6.5×10^{-2}	0.5×10^{-2}	*d*
25(DMPC)	88	26	36.1	0.9	*e*
25(DMPC)	200		3.5×10^{-1}		*f*
1 ($n = 2$)	90.3	26	2.6×10^{-2}	0.2×10^{-2}	*d*
2 ($m = n = 1$)			150–200		*e*
2 ($m = n = 2$)	115–130	26–35	20.5–31	0.3–0.6	*e*
2 ($m = n = 3$)	133–140	35–36	12.0–13.2	0.2–0.4	*e*

[a] Average diameter. [b] Standard deviation. [c] Average rate constant. [d] This work. [e] Ref. 10. [f] Ref. 2(*b*).

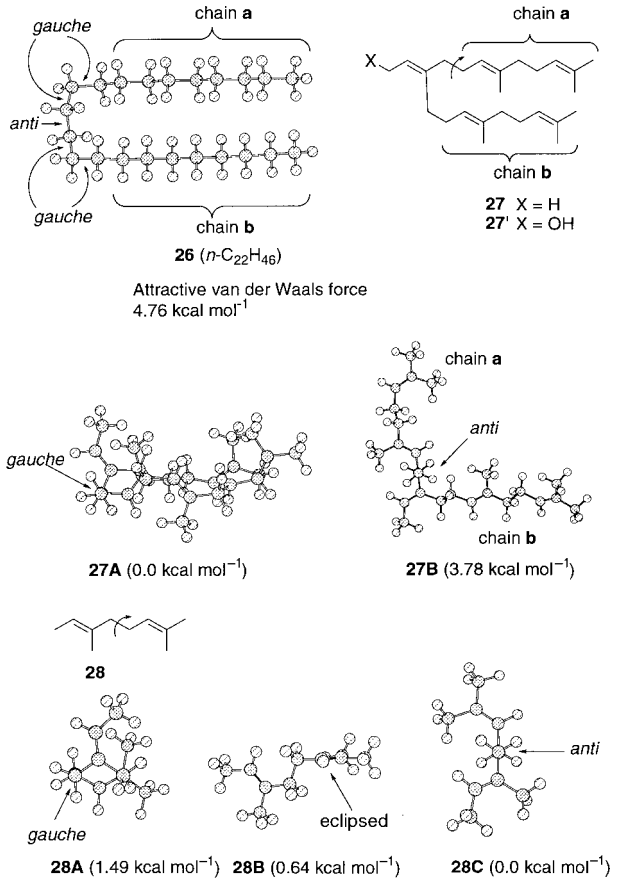

Fig. 8 Optimized structures of **26**, **27** and **28**, their relative energies (MM2) and the intramolecular van der Waals forces of **26** and **27**.

Recently Goodman has reported that the first alkane for which the hairpin conformation (see: conformer of docosane **26** in Fig. 8) is lower in energy than the extended one is octadecane, according to MM2 force field calculations.[15] The hairpin conformation is preferable because intramolecular attractive van der Waals forces outweigh the energetic cost of twisting the carbon chain away from the preferred extended *anti* conformation to the *gauche* conformation. A chain can be reversed with a combination of one *anti* and four *gauche* conformations. Following Goodman's protocol we calculated the attractive van der Waals forces of docosane **26**, whose carbon chain lengths (chains **a** and **b**) are comparable to those of **27**. The attractive van der Waals force of 4.76 kcal mol^{-1} can be obtained as the sum of the energy cost of twisting (=four times the energy difference between *anti* and *gauche*) and the difference in energy between extended and hairpin conformers.

Molecular mechanics and *ab initio* calculations have been employed to examine the phase conformation of prenyl derivatives in solution.[16] Exhaustive conformational searches were performed by varying all the dihedral angles (C–C–C–C and C=C–C–C) between −120 and 120° in two steps using the CAChe/Conflex system (optimized with molecular mechanics calculations, MM2).[17] The conformation searches of **27′** gave 2140 structures within 5.0 kcal mol^{-1} of the global minimum energy structure. The difference in energy between the folded conformer **27A** (global minimum conformer) and the extended conformer **27B** was found to be 3.78 kcal mol^{-1}. The conformer **27B** is transformed from **27A** by twisting a single bond in the chain **a** from *gauche* to *anti* (indicated by an arrow). The difference in energy between the *gauche* **28A** and *anti* **28C** conformers of 3,7-dimethyl-2,6-octadiene was calculated to be 1.49 kcal mol^{-1}. The attractive van der Waals force 5.27 kcal mol^{-1} obtained as the sum of the two energy differences was slightly higher than that of docosane **26**. The attractive van der Waals force decreased as the enthalpy of the conformer increased. Recently Gung *et al.* have reported an *ab initio* MO study of 1,5-hexadiene at the MP2/6-31G* level which shows that, unlike *n*-butane, there is little energy difference between the *anti* and the *gauche* conformations.[18] This indicates that the energies for the *gauche* conformations of **27**, **29** and **30** were overestimated. The attractive van der Waals forces are possibly weaker than those predicted using MM2 calculations.

Exhaustive conformation searches of **29** using the CAChe/Conflex system gave 568 structures within 5.0 kcal mol^{-1} of the global minimum energy structure. The intramolecular attractive van der Waals forces for the global minimum conformations **29A** (Fig. 9) and for octadecane were estimated to be 1.99 and 3.87 kcal mol^{-1}, respectively. The weaker intramolecular attractive force of **29** compared to that of octadecane shows a loosely packed state of the membranes of the 2-polyprenyl-substituted polyprenyl phosphates **6** and **8**. The larger attractive forces of **27A** (5.27 kcal mol^{-1}) and **30A** (3.58 kcal mol^{-1} obtained by the calculations shown in Fig. 10) imply that the interaction between the two alkenyl chains attached to the same sp^2 carbon atom is more effective. The vesicles of the phosphates **7** and **10** were less stable than those of the phosphate **20**. In the compounds **7** and **10** the polar head group is attached to the mobile unsaturated side chain **E**, whereas in the phosphate **20** the polar head group is attached directly to the rigid unit **A** composed of five carbon atoms (Fig. 11). The compact and rigid structure of **20** implies that the phosphate has a lower molecular volume and greater intermolecular attractive van der Waals interaction (as a result of a higher surface : volume ratio)[19] than those of 2-polyprenylpolyprenyl phosphates such as **6** and **8** (**D**). In these analyses the effects of solvent and of buffer components were

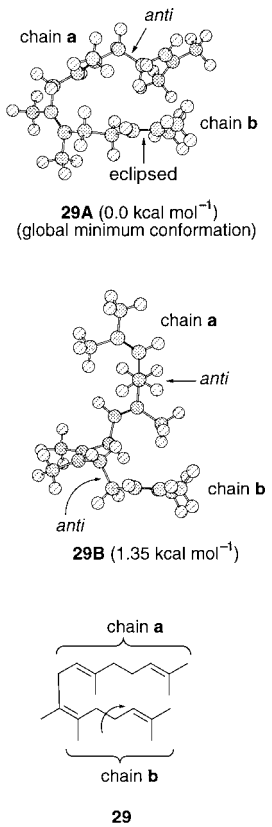

Fig. 9 Optimized structures of **29A** and **29**, their relative energies (MM2) and the intramolecular van der Waals force of **29**.

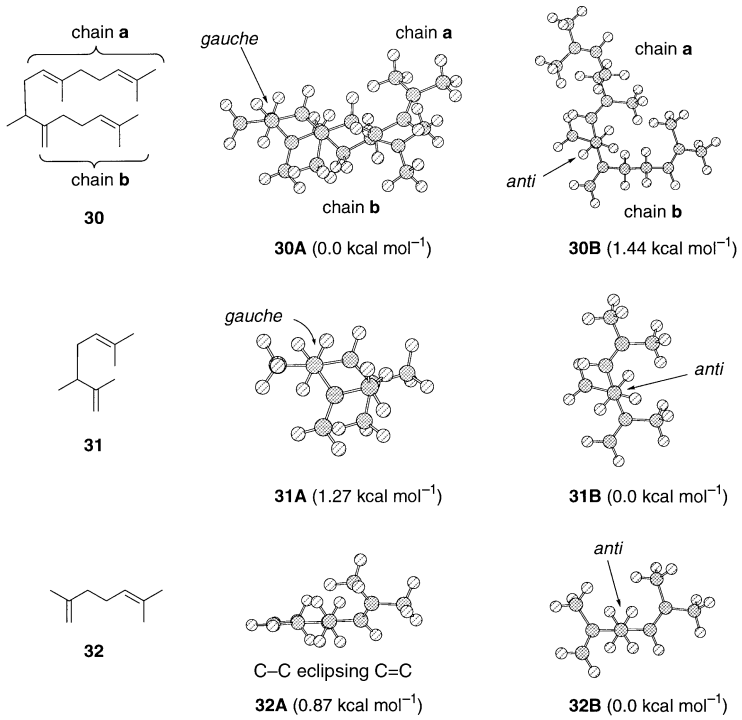

Fig. 10 Optimized structures of **30**, **31** and **32**, their relative energies (MM2) and the intramolecular van der Waals force of **30**.

ignored, but exclusion from water may be expected to compress and rigidify the folded hydrophobic system, favoring the smallest possible surface area.[15]

The fact that 6-polyprenyl-substituted polyprenyl phosphates form vesicles in a wide range of pH, unlike 2-polyprenyl-substituted polyprenyl phosphates (Table 1), indicates that the units **B** and **C** (**11**–**19**) are preferable to **D** and **E** (**6**–**10**) for vesicle formation. In the units **D** and **E** the polar head group and the junction of two chains are neighboring, whereas **B** and **C** possess a prenyl unit, as a spacer, between the polar head group and the junction. The vesicles of phosphate **20** possessing a rigid spacer (unit **A**) can be more tightly packed than those of 6-polyprenyl-substituted polyprenyl phosphates **11**–**19**.

The differences in vesicle formation between the 6-prenyl-substituted farnesyl phosphates **12** and **13** at pH 3.1 and between 6-farnesyl-substituted farnesyl phosphates **16** and **17**

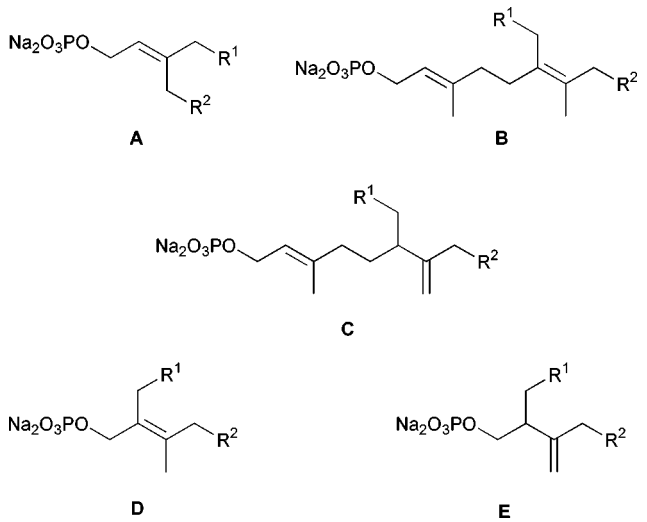

Fig. 11 Classification of substituted polyprenyl phosphates into five types of structures: **A** (compound **20**), **B** (compounds **12**, **14**, **16**, **19**), **C** (compounds **11**, **13**, **15**, **17**, **18**), **D** (compounds **6**, **8**, **9**), **E** (compounds **7**, **10**).

at pH 4.5 (see Table 1) suggest that the contribution of the hydrophobic region of the unit **C** is more important than that of unit **B**. As was discussed above, the unit **C** (corresponding to **30**: 3.58 kcal mol^{-1}) has a larger attractive van der Waals interaction than **B** (corresponding to **29A**: 1.99 kcal mol^{-1}). Therefore, for the formation of vesicles with phosphates **13** or **17**, an increase of their polar head region is needed. This could be obtained by increasing pH.

The dihedral angles C1–C2–C3–C4 and C3–C4–C5–C6 in a 1,5-hexadiene system are governed by a 1,3-allylic strain. To minimize this steric interaction these dihedral angles are expected to be 90°. In the chain **b** of the global minimum conformation **29A**, a less preferable C–C eclipsed form is present. This may be due to maximization of the attractive force between the chains **a** and **b**. The fact that unsaturated polyprenols are mobile unlike alkanes can be ascribed to the small rotational barrier of the C–C bond[14] and the presence of enormous structures within a small amount of energy of the global minimum energy structure.[18] Exhaustive conformation searches of **33** using the CAChe/Conflex system gave 2810 structures within 5.0 kcal mol^{-1} of the global minimum energy structure. Most of them, including the global minimum conformation (Fig. 12), were folded to maximize the attractive van der Waals interactions between the polyprenyl chains. The hydroxymethyl group is located inside the U-shaped polyprenyl chains. The conformational analysis indicates that the (2*Z*)-2-polyprenyl-substituted geranylgeranyl phosphates **21** and **22** can not form vesicles even if they adopt either the folded conformations similar to those of **33** or extended conformations. In fact, no vesicle formation was observed for **21** and **22**.

3.4 Structural parameters obtained from NMR spectral analysis

In order to reveal the conformation of the 1,4-pentadiene part of 2-polyprenyl-substituted polyprenols we needed to measure the dihedral angles C1–C2–C1′–C2′ and C2–C1′–C2′–C3′.[20] The numbering systems used to identify the carbon atoms are shown in Fig. 13. The first angle can be obtained from the

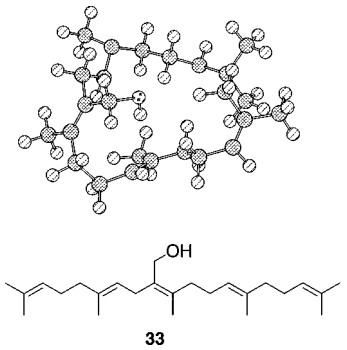

33

Fig. 12 Global minimum conformation of (2*Z*)-2-geranylfarnesol **33**.

spin coupling constant between C1 and C2′ using the Karplus relation. We have synthesized [1,2′-$^{13}C_2$]-2-farnesylfarnesol **44** (Scheme 1).[21] In the small scale synthesis we avoided using volatile prenylacetone as starting material and instead chose the less volatile geranylacetone **34**. The $^3J_{CC}$ coupling constant between the labeled carbon atoms is 0.77 Hz. The Karplus relation showed the dihedral angle C1–C2–C1′–C2′ to be near 90°. In this conformation the 1,3-allylic strain may be minimized. The measurement of the $^3J_{CC}$ coupling constant of the phosphate **46** was attempted in $CDCl_3$, but the signals were too broad to obtain the coupling constant, which is very small. The averaged value of the dihedral angles calculated for the 30 structures (67% total population) of 2-geranylfarnesol within 1.57 kcal mol^{-1} of the global minimum structure is 74°. In these polyprenols the 1,3-allylic strain may be one of the major factors governing their conformation.

For the fragment including terminal olefin C2–C1′–C2′=C3′ the Karplus relationship is not obeyed, due to hyperconjugative interaction at dihedral angles near 90°.[22] Instead of the dihedral angle, we can use the angle H1′–C1′–C2′–H2′ for the conformational analysis. The vicinal spin coupling constants (J = 6.9–7.3 Hz)[9a,c] between the 1′-H and 2′-H of the 2- and 6-polyprenyl-substituted polyprenols and their tetrabutylammonium phosphates are typical of free rotation.[20,23b] However, the vicinal coupling constants for the phosphates **6**, **8**, **9**, **12**, **14** and **16** were found to decrease with increasing chain length, *i.e.* the J values of **12**, **6**, **14**, **8** and **16** were 6.6, 6.4, 5.3, 4.4 and 4.0 Hz, respectively. Phosphates **12** and **6** having a small prenyl group may rotate freely (see also the T_1 maps in Fig. 14). The smaller J values for **14**, **8** and **16**, which have a larger substituent at C-2 or C-6 such as a geranyl or farnesyl group, can be ascribed to some hindered internal rotation due to the increase in the intramolecular attractive van der Waals forces. The vicinal spin coupling constants

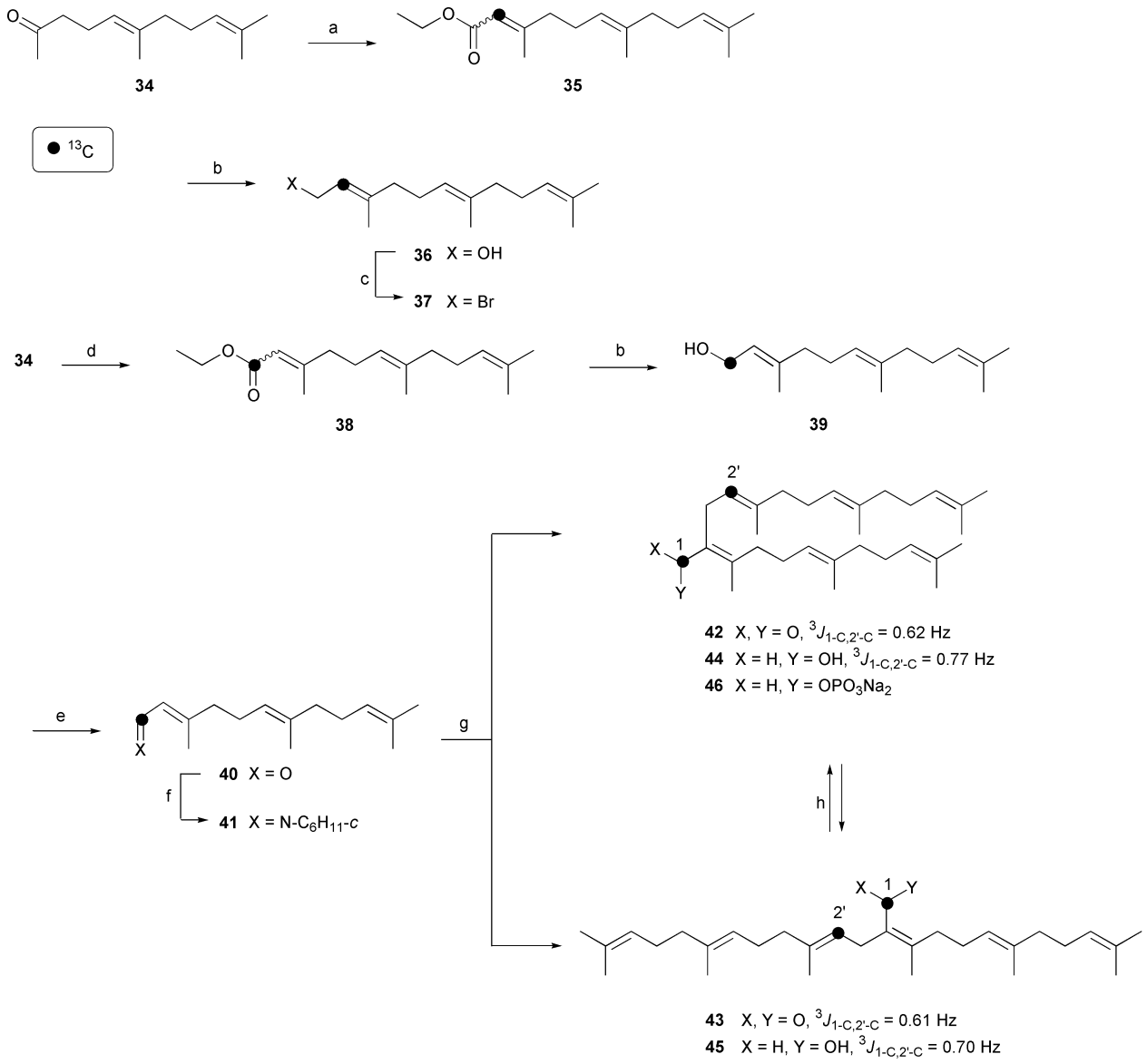

Scheme 1 Reagents: (a) $(EtO)_2P(=O)^{13}CH_2CO_2Et$, NaH; (b) Al^iBu_2H; (c) PBr_3, pyridine; (d) $(EtO)_2P(=O)CH_2{}^{13}CO_2Et$, NaH; (e) active MnO_2; (f) cyclohexylamine, K_2CO_3; (g) LiN^iPr_2, bromide **37**; (h) CF_3CO_2H, THF for the isomerization of *Z*-aldehyde **43** to *E*-aldehyde **42**.

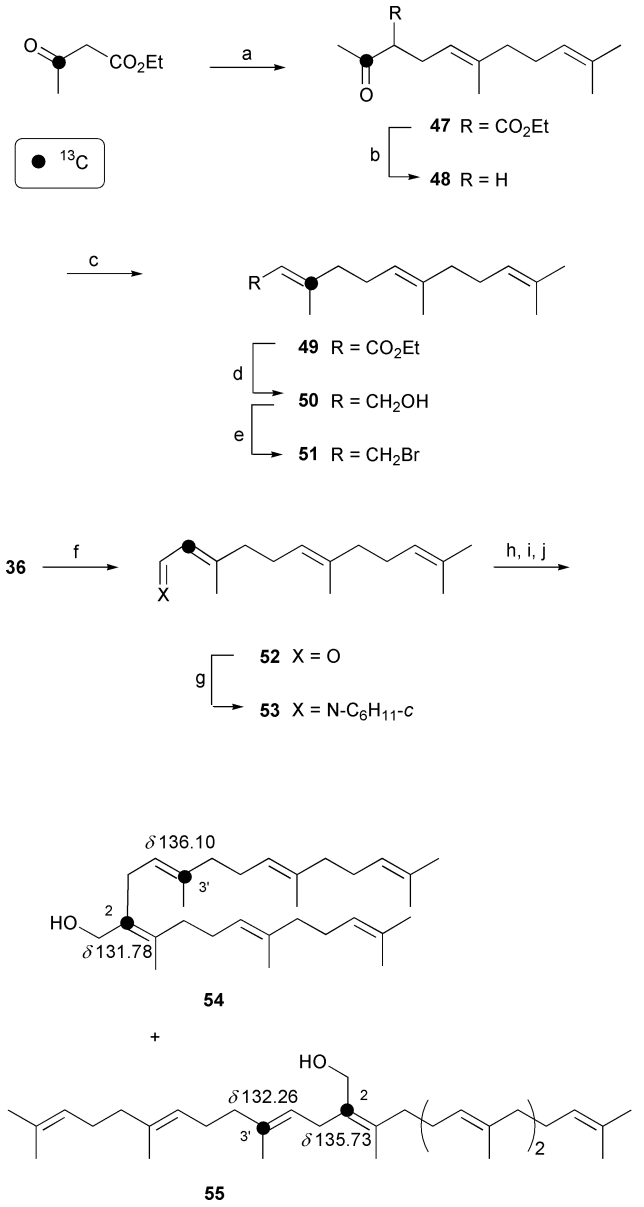

Scheme 2 Reagents: (a) NaH, geranyl bromide; (b) aq. NaOH then HCl; (c) $(EtO)_2P(=O)CH_2CO_2Et$, NaH; (d) Al^iBu_2H; (e) PBr_3, pyridine; (f) activated MnO_2; (g) cyclohexylamine, K_2CO_3; (h) LiN^iPr_2, bromide **51**; (h) CF_3CO_2H, THF for the isomerization of *Z*- to *E*-aldehyde.

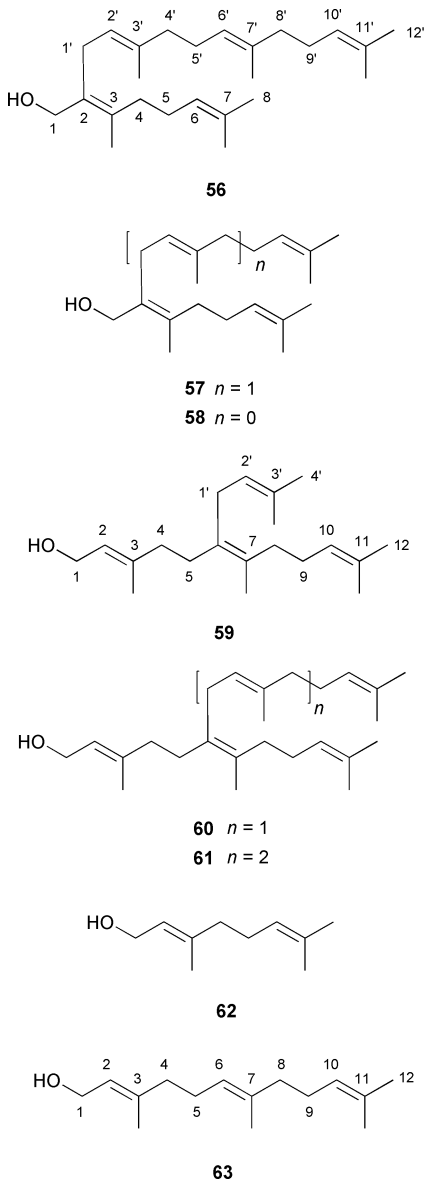

Fig. 13 Structures and numbering systems of **56**–**63**.

between the 1′-H and 2′-H of the (2*Z*)-phosphate **21** and the corresponding alcohol are 4.4 and 7.1 Hz, respectively.[9a] Viterbo and co-workers have reported the hindered internal rotation of the central C11–C12 bond in squalene ($J = 3.8$ Hz).[23b]

The assignment of the ^{13}C NMR spectra of polyprenols **56**–**61** was carried out independently from the T_1 measurement as much as possible, with the aid of the chemical shift values of ^{13}C-labeled compounds **44** and **54** (Schemes 1 and 2) and the known assignment of geraniol **62** and farnesol **63** (Fig. 13 and Table 3). 2-Polyprenylgeraniols **56** and **57** and 6-geranyl- and 6-farnesyl-geraniols **60** and **61** were freshly prepared following the procedures reported previously.[9a,c]

Firstly, the assignment of the ^{13}C NMR spectra of **56**–**58** was performed as follows. The signals observed in common in the spectra of **56**–**58** were assigned to the carbon atoms at C1–C12, 3-Me, 7-Me, 11-Me and C-1′. The four signals having nearly identical chemical shifts with those of the labeled carbons in **44** and **54** were assigned to C-1, C-2, C-2′ and C-3′. C-1′: the signals showing almost the same chemical shifts with that of C-1′ in **59** were assigned to C-1′ (*vide infra*). C-3: the chemical shift (δ 133.36) is slightly larger than those of terminal disubstituted olefinic carbons, *i.e.* C-7 in geraniol **62** and C-11 in farnesol **63** ordinarily resonating at δ *ca.* 131. C-4: the methylene carbon flanking the disubstituted olefinic carbon is observed at a higher field (*ca.* 5 ppm) than the corresponding methylene carbons in **62** and **63** due to the γ effect of the side chain *cis* to C-4. C-5, C-5′ and C-9′: the signals observed in common at δ *ca.* 26.8 in the spectra of **56**–**58** were assigned to the carbon atoms at C-5, and the other signals resonating at a slightly higher field were assigned to C-5′ of **56** and **57**. For farnesol **63**, the methylenic carbon atom C-5 resonates at a slightly higher field than the terminal methylenic carbon atom C-9. Based on this trend and with the aid of their T_1 values, the assignment of C-5′ and C-9′ in **56** was performed. C-6, C-6′ and C-10′: for farnesol **63**, the terminal monosubstituted olefinic carbon atom C-10′ resonates at a slightly lower field than the inner olefinic carbon atom C-7. The signal at δ 124.19 of **56**, which appears at a slightly lower field than those of the two other monosubstituted olefinic carbon atoms, is therefore assigned to the terminal olefinic carbon C-10′. The T_1 value of C-10′ being larger than those of the other two carbons supported the assignment.[22] C-6 and C-6′ were tentatively assigned. C-7 and C-11′: the resonances at δ 131.30 and 130.88 cannot be assigned unequivocally owing to their similar chemical shifts. The resonance (δ 130.88) possessing

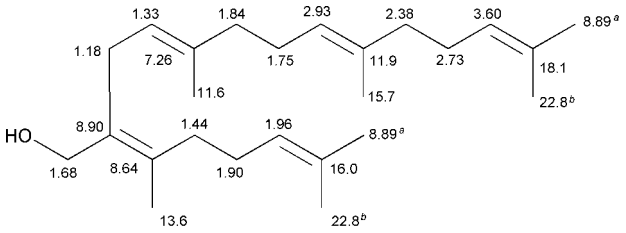

56

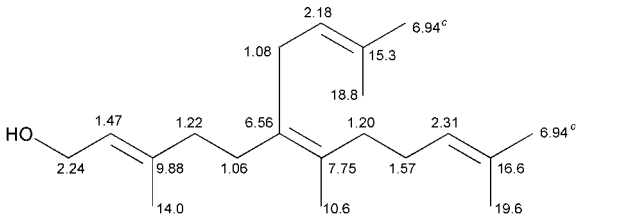

59

Fig. 14 Spin–lattice relaxation time NT_1 (in s) maps of the ^{13}C atoms of 2-farnesylgeraniol **56** and 6-prenylfarnesol **59**. Solutions of **56** (0.65 M) and **59** (0.82 M) in $CDCl_3$ were used for the measurements. N in NT_1 means the number of protons attached directly to a carbon atom.[a,b] The averaged NT_1 values for C-8 and C-12′ and 7-Me and C11′-Me.[c] The averaged NT_1 value for C-8 and C-12′.

larger T_1 must be assigned to the more mobile carbon, C-11′.[23] C-4′ and C-8′: for farnesol **63**, the methylenic carbon atom C-4 resonates at a slightly lower field than the methylenic carbon atom C-8. Based on the trend the assignment of C-4′ and C-8′ was performed. Methyl groups: the overlapping signal observed at δ 17.57 was assigned to the terminal *cis*-methyl carbon atoms, 7-Me and 11′-Me (see: 11-Me of farnesol **63**). The differentiation of 3-Me and 7′-Me was difficult (see also: 3-Me and 7-Me of **63**) and the assignment was achieved with the aid of their T_1 values. The remainder resonating at a lower field was assigned to 3′-Me.

The assignment of the ^{13}C NMR spectra of **59** was performed as follows. The carbon atoms C-1, C-2, C-3, C-4, C-9, 3-Me and 11-Me were assigned with the aid of the known assignment of geraniol **62** and farnesol **63**. The assignment of C-2, C-10, C-1′ and C-2′ was performed on the basis of their selective proton-decoupled spectra. Thus, the methylenic carbon C-5, whose chemical shift is slightly different, was assigned unequivocally. C-6 and C-7: the assignment was performed by comparing the chemical shifts with those of the tetraalkyl-substituted alkenes.[24] C-8: see the assignment of C-4 in **56**. C-11 and C-3′: the signals observed in common in the spectra of **59**–**61** were assigned to the carbon atoms at C-11. For **60** and **61**, see Experimental section. The chemical shift depended on the concentration of **59** and the δ value (131.22) of C-11 observed at lower concentration was slightly larger than that shown in Table 3.[9c] Based on the trend that the terminal methyl resonates at lower field than the inner methyl, we assigned 7-Me and 3′-Me.

3.5 Spin–lattice relaxation data

^{13}C Spin–lattice relaxation times T_1 can be a parameter of the flexibility of the 2- and 6-polyprenyl-substituted polyprenyl phosphates, although being qualitative.[25] We have measured the T_1 values of the 2-farnesyl-geraniol **56** and 6-prenyl-farnesol **59** (Fig. 14).[9c] In the former the tetrasubstituted double bond is rooted and the mobility of the main and side chains increased with increasing distance from C-2 and C-3, respectively. The relatively rigid structure of the central tetrasubstituted double bond part of the 6-prenylfarnesol **59** was indicated by the spin–lattice relaxation times. The vesicle for-

Table 3 ^{13}C NMR Chemical shifts of polyprenols **44**, **54**, **56**–**59**, **62** and **63**

	Chemical shift values, δ						
Carbon	**56**[a]	**57**	**58**	**59**[b]	**62**	**63**	**44**/**54**
2	131.81	131.83	132.06	123.13	123.40	123.8	131.78
3	133.36	133.76	133.82	139.17	138.20	139.5	
6	123.86[c]	124.07[d]	124.04	131.69	123.72	123.5	
7	131.30	131.60	131.77	128.75	131.11	135.3	
10				124.25		124.4	
11				130.84		131.2	
2′	122.94	122.99	122.99	123.44			122.92
3′	135.44	135.78	131.60	130.64			136.10
6′	124.00[c]	124.07[d]					
7′	134.80	131.45					
10′	124.19						
11′	130.88						
1	62.07	62.36	62.49	58.90	58.52	59.3	62.51
4	34.67	34.59	34.84	38.26	39.26	39.7	
5	26.87	26.77	26.93	31.07	26.12	26.4	
8	25.62[c]	25.59[d]	25.87	34.39	25.25	39.6	
9				27.04		26.8	
12				25.55[d]		25.6	
1	29.21	29.28	29.54	30.77			
4′	39.73	39.66	25.77	25.55[d]			
5′	26.53	26.48					
8′	39.66	25.59[d]					
9′	26.71						
12′	25.62[d]						
3-Me	16.04	15.95	17.70	16.13	15.80	15.9	
7-Me	17.57[d]	17.56	17.89	17.92	17.23	16.2	
11-Me				17.64		17.6	
3′-Me	17.97	17.95	18.12	17.43			
7′-Me	15.95	17.51					
11′-Me	17.57[d]						

[a] Obtained from a 0.65 M solution. [b] Obtained from a 0.82 M solution. [c] The assignment may be interchanged. [d] The peaks are overlapping.

mation of 6-polyprenyl-substituted polyprenyl phosphates **12**, **14** and **16** in the buffers with a wide range of pH may partly be attributed to the rigid structure.

These results from T_1 measurements show that the polyprenols **56** and **59** are more mobile in solution than their saturated counterparts such as phytol.[23c,26] The fact that the vesicles from unsaturated polyprenyl phosphates are less stable than those from their saturated counterparts can be interpreted based on the difference in the rigidity of the hydrophobic chains. To estimate experimentally the degree of contribution of the intramolecular attractive interaction to vesicle stabilization, we would require further systematic investigation on the spin–lattice relaxation times T_1 employing solutions of polyprenols and their phosphates with various chain lengths in polar and non-polar solvents.

Conclusion

The spontaneous vesicle formation of polyprenylated polyprenyl phosphates **6**–**20** and the structural properties of these amphiphiles and the corresponding alcohols have been reported. We now include these amphiphiles **6**–**19** as possible primitive biomembrane constituents to the hypothetical family tree of the chemical evolution of terpenoids as biomembrane constituents and reinforcers.[1b]

Acknowledgements

We are grateful for support granted by CNRS to S. G., Association "Amis des Sciences" to O. D. We thank Mr N. Midani for his technical assistance, Dr M. Tsuji, Nisshin Flour Milling, Dr T. Takigawa, Kuraray and Professor T. Eguchi, Tokyo Institute of Technology for their generous gifts of polyprenols.

References and notes

1 For reviews, see: (*a*) G. Ourisson and Y. Nakatani, *Chem. Biol.*, 1994, **1**, 11; (*b*) G. Ourisson and Y. Nakatani, *C. R. Acad. Sci. Ser. IIb*, 1996, **322**, 323; (*c*) G. Ourisson and Y. Nakatani, *Tetrahedron*, 2000, **55**, 3183.

2 (*a*) N. Plobeck, S. Eifler, A. Brisson, Y. Nakatani and G. Ourisson, *Tetrahedron Lett.*, 1992, **33**, 5249; (*b*) V. Birault, G. Pozzi, N. Plobeck, S. Eifler, M. Schmutz, T. Planché, J. Raya, A. Brisson, Y. Nakatani and G. Ourisson, *Chem. Eur. J.*, 1996, **2**, 789; (*c*) G. Pozzi, V. Birault, B. Werner, O. Dannenmuller, Y. Nakatani, G. Ourisson and S. Terakawa, *Angew. Chem., Int. Ed. Engl.*, 1996, **35**, 177; (*d*) O. Dannenmuller, K. Arakawa, T. Eguchi, K. Kakinuma, S. Blanc, A.-M. Albrecht, M. Schmutz, Y. Nakatani and G. Ourisson, *Chem. Eur. J.*, 2000, **6**, 645.

3 G. Ourisson and M. Rohmer, *Acc. Chem. Res.*, 1992, **25**, 403; (*b*) M.-A. Krajewski-Bertrand, A. Milon, Y. Nakatani and G. Ourisson, *Biochim. Biophys. Acta*, 1992, **1105**, 213.

4 G. Ourisson, *Pure Appl. Chem.*, 1989, **61**, 345; M. Keller, D. Hafenbradl, K. O. Stetter, G. Teller, Y. Nakatani and G. Ourisson, *Angew. Chem., Int. Ed. Engl.*, 1995, **34**, 1898.

5 For highly branched isoprenoid alkenes and alkanes isolated from sediments, see: J. K. Volkman, J. W. Farrington, R. B. Gagosian and S. G. Wakeham, in *Advances in Organic Geochemistry 1981*, ed. M. Bjoroy, Wiley, Chichester, 1983, pp. 228–240; J. N. Robson and S. J. Rowland, *Nature* (*London*), 1986, **324**, 561; S. J. Hird, R. Evans and S. J. Rowland, *Mar. Chem.*, 1992, **37**, 117; S. T. Belt, D. A. Cooke, S. J. Hird and S. Rowland, *J. Chem. Soc., Chem. Commun.*, 1994, 2077; M. J. L. Hoefs, J. S. S. Damsté and J. W. de Leeuw, *Org. Geochem.*, 1995, **23**, 263; Y. Huang, M. Murray, G. Eglinton and P. Metzger, *Tetrahedron Lett.*, 1995, **36**, 5973; M. J. Rospondek, J. Koster and J. S. Sinninghe Damste, *Org. Geochem.*, 1997, **26**, 295.

6 For highly branched isoprenoid alkenes and alkanes isolated from diatomaceous algae, see: S. J. Rowland and J. N. Robson, *Mar. Environ. Res.*, 1990, **30**, 191; R. E. Summons, R. A. Barrow, R. J. Capon, J. M. Hope and C. Stranger, *Aust. J. Chem.*, 1993, **46**, 907; J. K. Volkman, S. M. Barrett and G. A. Dunstan, *Org. Geochem.*, 1994, **21**, 407; S. T. Belt, D. A. Cooke, J.-M. Robert and S. Rowland, *Tetrahedron Lett.*, 1996, **37**, 4755; E. J. Wraige, S. T. Belt, C. A. Lewis, D. A. Cooke, J. M. Robert, G. Masse and S. J. Rowland, *Org. Geochem.*, 1997, **27**, 497; E. J. Wraige, L. Johns, S. T. Belt, G. Massé, J.-M. Robert and S. J. Rowland, *Phytochemistry*, 1998, **51**, 69; E. J. Wraige, S. T. Belt, G. Massé, J.-M. Robert and S. J. Rowland, *Org. Geochem.*, 1998, **28**, 855; J. S. S. Damsté, W. I. C. Rijpstra, S. Schouten, H. Peletier, M. J. E. van der Maarel and W. W. C. Gieskes, *Org. Geochem.*, 1999, **30**, 95; L. Johns, E. J. Wraige, S. T. Belt, C. A Lewis, G. Masse, J. M. Robert and S. J. Rowland, *Org. Geochem.*, 1999, **30**, 1471; J. S. S. Damsté, S. Schouten, W. C. Rijpstra, E. C. Hopmans, H. Peletier, W. W. C. Gieskes and J. A. J. Geenevasen, *Org. Geochem.*, 1999, **30**, 1581; S. T. Belt, G. Allard, G. Massé, J.-M. Robert and S. Rowland, *Chem. Commun.*, 2000, 501; S. J. Rowland, D. A. Yon, C. A. Lewis and J. R. Maxwell, *Org. Geochem.*, 1985, **8**, 207; C. Porte, D. Barceló, T. M. Tavares, V. C. Rocha and J. Albaigés, *Arch. Environ. Contam. Toxicol.*, 1990, **19**, 263; S. J. Rowland, S. T. Belt, E. J. Wraige, G. Massé, C. Roussakis and J.-M. Robert, *Phytochemistry*, 2001, **56**, 597.

7 For highly branched polyprenols and related alcohols isolated from higher plants, see: E. Lemmich, *Phytochemistry*, 1979, **18**, 1195; H. Nagano, M. Tori, M. Shiota and J. de Pascual Teresa, *Bull. Chem. Soc. Jpn.*, 1984, **57**, 2971; M. Bruno, L. Lamartina, F. Lentini, C. Pascual and G. Savona, *Tetrahedron Lett.*, 1984, **25**, 4287; L. Mangoni, D. Merola, P. Monaco, M. Parrilli and L. Previtera, *Tetrahedron Lett.*, 1984, **25**, 2597; C. Porte, D. Barceló, T. M. Tavares, V. C. Rocha and J. Albaigés, *Arch. Environ. Contam. Toxicol.*, 1990, **19**, 263; J.-L. Giner, J. D. Berkowitz and T. Andersson, *J. Nat. Prod.*, 2000, **63**, 267; S. Faure, J. D. Connolly, C. O. Fakunle and O. Piva, *Tetrahedron*, 2000, **56**, 9647; H. R. Nawaz, A. Malik and M. S. Ali, *Phytochemistry*, 2001, **56**, 99.

8 For highly branched polyprenyl acetate isolated from higher plants, see: M. J. Gieselmann, D. S. Moreno, J. Fargerlund, H. Tashiro and W. L. Roelofs, *J. Chem. Ecol.*, 1979, **5**, 27.

9 (*a*) H. Nagano and K. Kudo, *Bull. Chem. Soc. Jpn.*, 1996, **69**, 2071; (*b*) H. Nagano, T. Nagasawa and M. Sakuma, *Bull. Chem. Soc. Jpn.*, 1997, **70**, 1969; (*c*) H. Nagano, E. Nakanishi, S. Takajo, M. Sakuma and K. Kudo, *Tetrahedron*, 1999, **55**, 2591.

10 H. Goto and E. Osawa, *J. Am. Chem. Soc.*, 1989, **111**, 8950; H. Goto and E. Osawa, *J. Chem. Soc., Perkin Trans. 2*, 1993, **187**; JCPE, P040 and P021, OCPE, no. 59, developed by H. Goto and E. Osawa.

11 J. N. Israelachvili, *Intermolecular and Surface Forces*, Academic Press, London, 1994, pp. 380–382; J. N. Israelachvili, S. Marcelja and R. G. Horn, *Q. Rev. Biophys.*, 1989, **13**, 121; P. R. Cullis and B. De Kruijff, *Biochim. Biophys. Acta*, 1979, **559**, 99.

12 A. Milon, T. Lazrak, A.-M. Albrecht, G. Wolff, G. Weill, G. Ourisson and Y. Nakatani, *Biochim. Biophys. Acta*, 1986, **859**, 1.

13 Y. Nagawa and S. L. Regen, *J. Am. Chem. Soc.*, 1992, **114**, 1668.

14 M. J. S. Dewar and M. C. Kohn, *J. Am. Chem. Soc.*, 1972, **94**, 2699; E. L. Eliel and S. H. Wilen, *Stereochemistry of Organic Compounds*, John Wiley & Sons, Inc., New York, 1994, p. 615.

15 J. M. Goodman, *J. Chem. Inf. Comput. Sci.*, 1997, **37**, 876.

16 J. L. Broeker, R. W. Hoffmann and K. N. Houk, *J. Am. Chem. Soc.*, 1991, **113**, 5006; N. J. Murgolo, A. Patel, S. S. Stivala and T. K. Wong, *Biochemistry*, 1989, **28**, 253.

17 H. Goto and E. Osawa, *J. Am. Chem. Soc.*, 1989, **111**, 8950; H. Goto and E. Osawa, *J. Chem. Soc., Perkin Trans. 2*, 1993, 187.

18 B. W. Gung, Z. Zhu and R. A. Fouch, *J. Am. Chem. Soc.*, 1995, **117**, 1783; K. B. Wiberg and M. A. Murcko, *J. Am. Chem. Soc.*, 1988, **110**, 8029.

19 E. L. Eliel and S. H. Wilen, *Stereochemistry of Organic Compounds*, John Wiley & Sons, Inc., New York, 1994, p. 600.

20 B. Lemarie and B. Braillon, *J. Magn. Reson.*, 1979, **35**, 343.

21 T. J. Zahn, M. B. Ksebati and R. A. Gibbs, *Tetrahedron Lett.*, 1998, **39**, 3991.

22 J. M. Marshall, *Carbon-carbon and carbon-proton NMR couplings: Applications to organic stereochemistry and conformational analysis*, Verlag Chemie International, Deerfield Beach, FL, USA, 1983, pp. 65–122.

23 (*a*) R. A. Goodman, E. Oldfield and A. Allerhand, *J. Am. Chem. Soc.*, 1973, **95**, 7553; (*b*) L. Pogliani, M. Ceruti, G. Ricchiardi and D. Viterbo, *Chem. Phys. Lipids*, 1994, **70**, 21; (*c*) J. M. Brown and D. R. M. Martens, *Tetrahedron*, 1977, **33**, 931.

24 P. A. Couperus, A. D. H. Clague and J. P. C. M. van Dongen, *Org. Magn. Reson.*, 1976, **8**, 426.

25 E. Breitmaier, K.-H. Spohn and S. Berger, *Angew. Chem., Int. Ed. Engl.*, 1975, **14**, 144.

26 The T_1 values of the terminal *trans*-methyls, which are near the axis, were smaller than those of the corresponding terminal *cis*-methyls. A. Okubo, H. Kawai, T. Matsunaga, T. Chuman, S. Yamazaki and S. Toda, *Tetrahedron Lett.*, 1980, **21**, 4095.